

# Striatal indirect pathway mediates exploration via collicular competition

<https://doi.org/10.1038/s41586-021-04055-4>

Jaeon Lee<sup>1</sup> & Bernardo L. Sabatini<sup>1</sup>✉

Received: 5 October 2020

Accepted: 27 September 2021

Published online: 03 November 2021

 Check for updates

The ability to suppress actions that lead to a negative outcome and explore alternative actions is necessary for optimal decision making. Although the basal ganglia have been implicated in these processes<sup>1–5</sup>, the circuit mechanisms underlying action selection and exploration remain unclear. Here, using a simple lateralized licking task, we show that indirect striatal projection neurons (iSPN) in the basal ganglia contribute to these processes through modulation of the superior colliculus (SC). Optogenetic activation of iSPNs suppresses contraversive licking and promotes ipsiversive licking. Activity in lateral superior colliculus (ISC), a region downstream of the basal ganglia, is necessary for task performance and predicts lick direction. Furthermore, iSPN activation suppresses ipsilateral ISC, but surprisingly excites contralateral ISC, explaining the emergence of ipsiversive licking. Optogenetic inactivation reveals inter-collicular competition whereby each hemisphere of the superior colliculus inhibits the other, thus allowing the indirect pathway to disinhibit the contralateral ISC and trigger licking. Finally, inactivating iSPNs impairs suppression of devalued but previously rewarded licking and reduces exploratory licking. Our results reveal that iSPNs engage the competitive interaction between ISC hemispheres to trigger a motor action and suggest a general circuit mechanism for exploration during action selection.

Activities of direct- and indirect-pathway striatal projection neurons (dSPN and iSPN, respectively) are thought to reinforce and punish actions associated with good and bad outcomes, respectively<sup>6–9</sup>. iSPN activation can also acutely suppresses movement<sup>2,6,10–13</sup>. To examine whether iSPNs also mediate exploration, we measured the behavioural consequences of transiently activating iSPNs in thirsty mice performing a licking task for water rewards. Mice were trained on a lateralized licking task in which a brief (50 ms) auditory cue (tone A or tone B) indicated the spout (left or right) at which a lick would trigger a water reward (Fig. 1a, b, Extended Data Fig. 1a). We categorized the outcome of each trial, on the basis of the timing and direction of the first lick (the ‘choice’ lick), as either correct (rewarded with water), incorrect or miss (no licks within 500 ms after tone onset) (Extended Data Fig. 1b, c).

We activated iSPNs in eight striatal regions on separate trials (four sites per fibre) on the right side of the brain. Brief unilateral iSPN stimulation immediately after tone onset decreased the fraction of correct outcomes (Fig. 1d, e). The effect was specific to ventrolateral striatum (VLS) during left-cued (contralateral) trials, which induced errors consisting largely of incorrect choice licks to the right (ipsilateral) side (Fig. 1e, f, Extended Data Fig. 1d). The outcomes of left-cued trials following the stimulation trial were unaffected, indicating that the stimulation protocol did not cause a persistent change in behaviour or action value<sup>2,7</sup> (Extended Data Fig. 1e). When mice selected the correct spout despite the stimulation, licks were delayed relative to control trials, suggesting that iSPNs might also control lick timing<sup>11</sup> (Extended Data Fig. 1f).

Ipsiversive licking after iSPN activation could result from inhibiting contraversive licking, or promoting ipsiversive licking. To distinguish these, we devalued the right spout by omitting the reward even after correct choices (Extended Data Fig. 2a, d). The mice with bilateral tapered fibres targeting each VLS were trained to perform the main task, and optogenetically stimulated before and after extinction of the right spout (Extended Data Fig. 2a, c). Pre-extinction stimulation of left VLS produced incorrect licking, consistent with the effects reported above (Extended Data Fig. 2a). After extinction, mice no longer licked to the devalued spout in no-stimulation right-cued trials, causing an increase in the fraction of miss trials (Extended Data Fig. 2a). However, iSPN stimulation in the left VLS during right-cued trials caused mice to lick to the left (ipsilateral) spout (Extended Data Fig. 2a, b). This suggests that ipsiversive licking triggered by iSPN stimulation is not purely the consequence of suppressing licking to the contralateral side and indicates that iSPNs can trigger a learned motor action. By contrast, stimulating iSPNs in the right VLS lost its ability to trigger ipsiversive licking after extinction, suggesting that iSPN stimulation causes mice to switch to an alternative ipsiversive motor programme only if it is a valuable option (Extended Data Fig. 2c, d). Bilateral iSPN stimulation increased misses but not incorrect choices, indicating that action switching is a unique consequence of unilateral iSPN stimulation (Extended Data Fig. 2c). Overall, these and further results (Extended Data Fig. 2f–h) indicate that unilateral iSPN activation can cause ipsiversive licking, if it is a reinforced motor programme, and even in the absence of contraversive licking suppression. Notably, inactivation

<sup>1</sup>Howard Hughes Medical Institute, Department of Neurobiology, Harvard Medical School, Boston, MA, USA. ✉e-mail: bsabatini@hms.harvard.edu

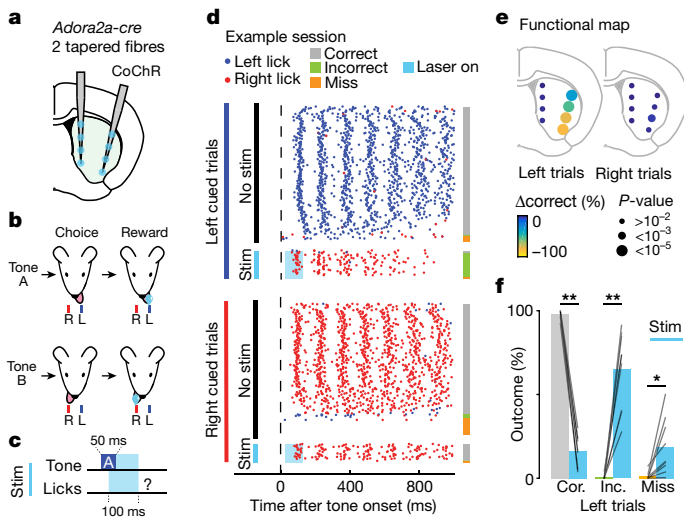


**Fig. 1 | iSPN activation in ventrolateral striatum induces ipsiversive movements.** **a**, Stimulation protocol: CoChR (green) was expressed in *Adora2a-cre* mouse, which was implanted with two tapered fibres. Each circle (blue) indicates a stimulation site. **b**, Trial structure of the lateralized licking task. L, left; R, right. **c**, Example stimulation protocol shown for left cued (tone 'A') trial: the laser (light blue) is turned on in a random subset (approximately 30%, left and right) of trials for 100 ms starting 25 ms after tone onset. Stim, stimulation. **d**, Each row shows behaviour in a single trial with each dot representing a lick to the left (blue) or right (red) port timed relative to tone onset. Trials are sorted by trial type (top: left-cued trials; bottom: right-cued trials) and further divided into no-stimulation trials (black) and optogenetic stimulation trials (light blue). The far-right column shows the trial outcomes labelled as correct (grey), incorrect (green) or miss (orange). **e**, Summary of functional perturbations (percentage of correct choices,  $\Delta$ correct) induced by optogenetic stimulation on left- or right-cued trials. Each circle indicates a striatal stimulation site with the colour and size denoting the effect size and *P*-value (bootstrap), respectively ( $n = 5$  mice, 9 sessions). Stimulation in the VLS most perturbed performance ( $\Delta$ correct = -82%,  $P < 10^{-5}$ ). **f**, Trial outcomes with and without VLS stimulation ( $n = 9$  sessions) showing that stimulation (light blue bars) significantly decreased correct (cor.) (grey), and increased incorrect (inc.) (green) and miss (orange) rates (\* $P < 0.01$ , \*\* $P < 0.001$ ; two-tailed *t*-test).

of dSPNs did not mimic iSPN activation as it induced misses on both contraversive and ipsiversive cued trials (Extended Data Fig. 3).

### Bilateral push-pull modulation of ISC

The superior colliculus (SC) is a brain region that is downstream of basal ganglia, and is implicated in decision making and choice competition<sup>14–20</sup>, and is necessary for licking behavior<sup>21</sup>. We hypothesized that the behavioural phenotype induced by iSPN stimulation might arise from modulation of ISC activity. Consistent with this hypothesis, SNr neurons downstream of VLS (<sup>VLS</sup>SNr) bilaterally innervate contralateral and ipsilateral ISC<sup>22</sup>, regions whose activity is necessary for contraversive licking in our task (Extended Data Fig. 4).

To uncover the effect of iSPN activation on ISC, we used multi-electrode silicon probes to record from ISC in mice performing the task and stimulated right VLS iSPNs in a random subset of trials. In trials without stimulation, activity of individual ISC units displayed trial-type selectivity for lick direction (Fig. 2b). Mean selectivity (the difference in activities in trials cued to preferred versus non-preferred directions) emerged gradually after tone onset and was maintained before the first lick, indicating that ISC has information that could drive the upcoming lick direction (Fig. 2c). As a population, ISC neurons fired more during contraversive than ipsiversive trials, and twice as many units were contraversive than ipsiversive lick-preferring (Extended Data Fig. 4e–j). Thus, ISC activity is higher before and during contraversive

licking, consistent with ISC involvement in generating contraversive licking.

During stimulation trials, units in the right ISC were suppressed by right iSPN stimulation whereas in the left ISC units were excited by the stimulation (Fig. 2d–g) (some units on both sides remained unaffected; Extended Data Fig. 5a). The effect of iSPN activation was stronger in left-cued trials during which behaviour was affected. The stimulation also specifically modulated contraversive lick-preferring units but not ipsiversive lick-preferring units, consistent with the function of ISC in driving contraversive licking (Extended Data Fig. 5b, d), and suggesting a high-degree of synaptic specificity within nuclei innervated by basal ganglia outputs.

In a subset of sessions, stimulation caused enough of both incorrect and miss trials to compare the activity in these two kinds of errors. In those sessions, we found that left SC, but not right SC activity during stimulation predicted behavioural outcome, with higher firing rates during incorrect licking compared with during miss trials (Extended Data Fig. 5c). In a subset of mice (four out of seven), we also stimulated iSPNs during the inter-trial interval (ITI), which occasionally triggered licks to the ipsilateral side (Extended Data Fig. 2h). We observed a similar pattern of inhibition and excitation of ISC hemispheres when the stimulation was applied during the ITI, with activity in left SC differentiating behavioural outcome (Extended Data Fig. 5e–g). Overall, iSPN activation caused push-pull modulation of ISC hemispheres, with the magnitude of contralateral ISC excitation predicting the behavioural outcome after stimulation.

### Competition between ISC hemispheres

We hypothesized that ISC in one hemisphere tonically suppresses ISC in the other, forming a competitive network, such that inhibiting one ISC via iSPN activation might disinhibit the opposite ISC. Consistent with this hypothesis, we first confirmed the existence of an interhemispheric projection between ISCs (Extended Data Fig. 6a). Furthermore, brief unilateral inhibition of right ISC with an inhibitory opsin (Jaws; 400-ms pulse starting 25 ms after tone onset delivered randomly in about 20% of trials) recapitulated the incorrect licking phenotype observed following iSPN activation (Fig. 3a, b, Extended Data Fig. 6b). Surprisingly, similar inhibition of the intermediate reticular formation (IRt), a region downstream of <sup>VLS</sup>SNr, failed to increase incorrect licking, but instead increased misses on both left- and right-cued trials (Extended Data Fig. 6c–f). These results suggest that ISC, but not IRt, mediates the effect of iSPN activation.

To functionally confirm the existence of inter-ISC competitive interactions, we performed extracellular recordings in ISC while unilaterally inhibiting the right ISC (Fig. 3c). Jaws activation reliably suppressed activity in the illuminated region (Extended Data Fig. 6g–i) and, consistent with inter-ISC competition, increased activity in the left (contralateral) ISC (Fig. 3d, e). The effect was stronger during left trials, specific to contraversive-preferring units, and magnitude of the effect predicted behavioral outcomes, in a similar fashion as that observed after iSPN activation (Fig. 3d, e, Extended Data Fig. 6j, k). Overall, ISC inhibition recapitulated the behavioral and neural phenotypes induced by iSPN activation.

### iSPN activity is necessary for lose-switch behaviour

As iSPNs are activated during negative outcomes<sup>3,23</sup>, we hypothesized that iSPN activity might be necessary for 'lose-switch' behaviour, namely to suppress unrewarded actions while switching to an alternative action. To test this hypothesis, we inactivated iSPNs in mice expressing the inhibitory opsin GtACR1 in the indirect pathway<sup>24</sup> (*R26-CAG-LNL-GtACR1-ts-FRed-Kv2.1; Adora2a-cre*) (Extended Data Fig. 7a). We compared the effect of right VLS iSPN inactivation during normal task performance (baseline session) and after omitting rewards on the

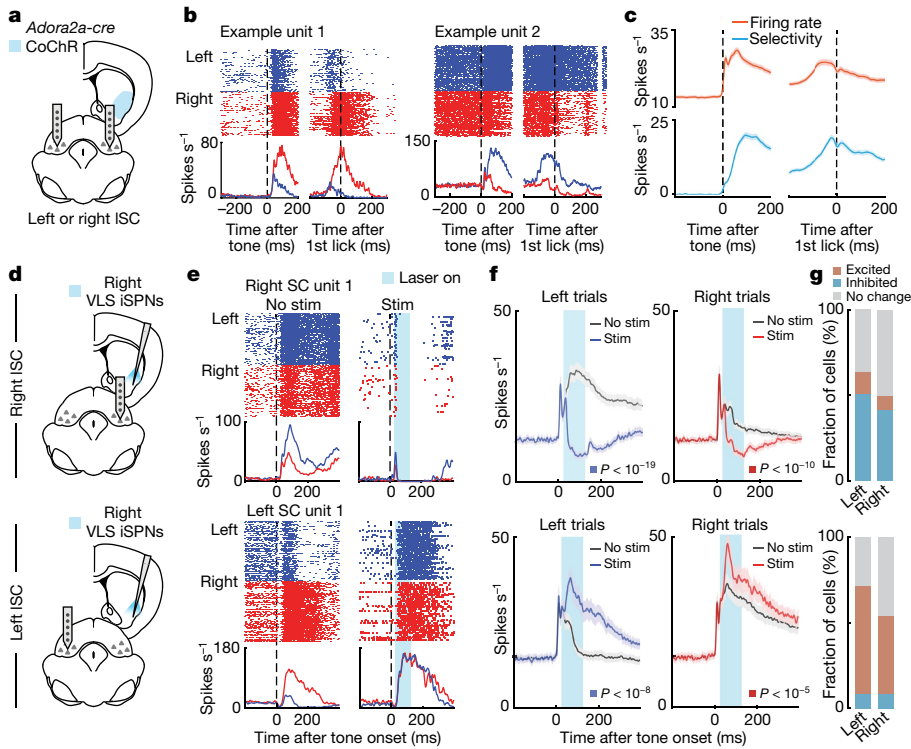


**Fig. 2 | Bilateral and opposite modulation of ISC hemispheres by iSPN activation.** **a**, Schematic of extracellular recording in ISC on either side of the brain in *Adora2a-cre* mice expressing CoChR in VLS and performing the task. **b**, Peri-stimulus time histogram of activities of two example units. Correct left (blue) and right (red) cued trials are shown, aligned to either tone onset or the first lick (dashed lines). **c**, Mean firing rate (orange) and firing rate selectivity (light blue) aligned to tone onset and first lick (dashed lines). Solid line shows the mean and shaded areas indicate the s.e.m. across units ( $n = 673$  units, 7 mice). **d**, Schematic of stimulation of iSPN in the right VLS while recording in the right (top) or left (bottom) ISC. **e**, Peri-stimulus time histograms of activities for two example units recorded in either right (top) or left (bottom) ISC in left- (blue) and right- (red) cued trials either without (no stim, left) or with (stim, right) optogenetic stimulation (light blue). **f**, Average firing rate of ISC

units in the right (top) and left (bottom) ISC during left- (blue) and right- (red) cued trials (stimulation in blue or red; no stimulation in grey). Only units that had directional selectivity during no stimulation trials are shown (right SC:  $n = 249$ , left SC:  $n = 186$ ). Stimulation decreased activity of neurons in the right SC (left trials:  $P < 10^{-19}$ , right trials:  $P < 10^{-10}$ ; two-tailed *t*-test) and increased activity of neurons in the left SC (left trials:  $P < 10^{-8}$ , right trials:  $P < 10^{-5}$ ; two-tailed *t*-test comparing average activity during the 100 ms of stimulation). **g**, Fractions of units that were significantly modulated. Cells were excited (red), inhibited (blue) or showed no change (grey). There were more inhibited than excited units in right SC (left trial:  $P < 10^{-10}$ , right trial:  $P < 10^{-10}$ ; two-tailed binomial test), and more excited than inhibited units in the left SC (left trial:  $P < 10^{-26}$ , right trials:  $P < 10^{-15}$ ; two-tailed binomial test).

left spout (extinction session) (Fig. 4a). iSPN activity was not required for correct licking to the contralateral spout during the baseline session (Fig. 4b, c). During extinction day 1, mice learned to suppress the unrewarded action (left licks) by increasing miss trials and also explored the right spout by increasing incorrect trials, even though right licks during left-cued trials were never rewarded. Inactivating iSPN impaired the ability to suppress left licks, and reduced exploratory licking to the right side (Fig. 4b, c). Exploration of the right port during left-cued trials decreased over days, suggesting the existence of another mechanism underlying suppression of exploratory licks that were never rewarded (Extended Data Fig. 7c). Right iSPN inactivation during the baseline session also impaired normal performance on right trials (non-devalued side), suggesting that iSPNs suppress off-target actions (Extended Data Fig. 7b).

To understand the electrophysiological correlates of these effects, we recorded activity in left or right ISC after mice had undergone extinction (Fig. 4d, f). iSPN inhibition caused robust excitation on the right (ipsilateral) and inhibition on the left (contralateral) ISC in the first 100 ms window during inactivation, the opposite of what was observed with iSPN activation (Fig. 4e, g, Extended Data Fig. 7e). Changes in activity in ISC in each hemisphere in optogenetic suppression trials predicted the behavioural outcome, suggesting a causal role of ISC in driving behaviour (Extended Data Fig. 7f, g). Furthermore, optogenetic gain and loss of iSPN activity pushed ISC population activity selectively

along the dimension that best discriminated upcoming lick choice (Extended Data Figs. 8, 9). Thus, iSPN activity is necessary to implement ‘lose-switch’ behaviour via bilateral modulation of ISC dynamics.

## Discussion

Although many studies have optogenetically activated iSPNs and reported behavioural consequences, only a few have simultaneously recorded downstream activity to understand the impact of the manipulation<sup>6,8,12</sup>. We found that iSPN activation excites neurons in the contralateral ISC, indicating that the effect of iSPN activity on downstream areas is more complex than predicted by classic models of the basal ganglia.

Mechanistically, given the direct connection between ISC hemispheres, long-range inhibitory projections or excitatory projections innervating local inhibitory neurons could mediate the excitatory effect<sup>25–29</sup>. An intermediate region outside colliculus could also mediate this effect<sup>30,31</sup>. In addition, the <sup>VLS</sup>Nr projection to the contralateral ISC that we described could also contribute<sup>32,33</sup> (Extended Data Fig. 10a–d).

Although we studied lateralized action selection, it is possible that a similar mechanism for exploration might exist for pairs of categorically different actions (for example, licking versus locomotion). Previous studies have found switching between non-lateralized actions by activating iSPNs<sup>3,34,35</sup>. One possibility is that distinct regions within SC

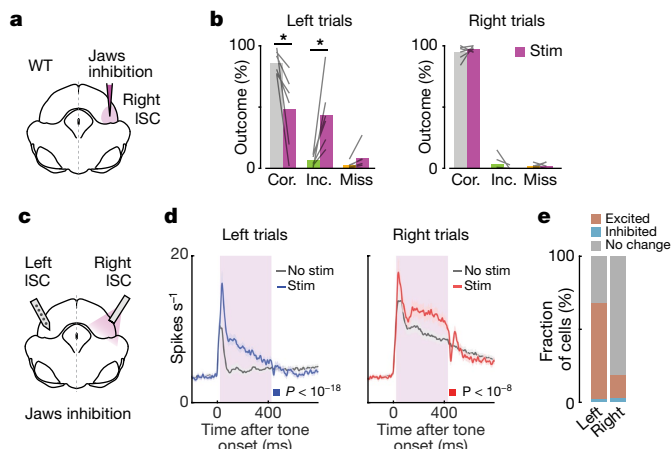


**Fig. 3 | Unilateral inhibition of ISC mimics iSPN activation.** **a**, Schematic illustrating Jaws expression in the right ISC in wild-type (WT) mice. **b**, ISC inhibition caused a significant decrease in correct rate, and a significant increase in incorrect rates ( $*P < 0.05$ , two-tailed  $t$ -test) in left trials ( $n = 6$  mice). **c**, Schematic illustrating the optical fibre in the right ISC and recording electrode in the left ISC. **d**, Mean firing rate of all left ISC units in left- (left) and right- (right) cued trials with (blue and red) and without (grey) stimulation ( $n = 152$  units, 4 mice). The laser-on period is shown in purple. Stimulation (right ISC inactivation) increased firing rate for both left and right trials (left trials:  $P < 10^{-18}$ , right trials:  $P < 10^{-8}$ ; two-tailed  $t$ -test). Only directionally selective units are shown. **e**, Fractions of units that were significantly excited (red) or inhibited (blue) and that were unaffected (grey). There were more excited than inhibited units (left trials:  $P < 10^{-99}$ , right trials:  $P < 10^{-3}$ ; two-tailed binomial test).

represent distinct actions and receive input from distinct basal ganglia topographical zones, such that competition between categorically different actions might occur locally within one SC hemisphere.

Previous studies have shown that iSPNs are preferentially active after mice experience negative outcomes<sup>3,23,36</sup>. Thus, we propose that the function of iSPNs is to drive exploration after the occurrence of a negative outcome (Extended Data Fig. 10). In this model, the ‘negative reward prediction error’ signalled by dips in dopamine neuron activity and concentration<sup>37,38</sup> strengthens inputs onto iSPNs<sup>39–41</sup> such that the subsequently increased iSPN activity more effectively suppresses the corresponding action. If SC tracks all the actions available to an animal, iSPN suppression of one action in SC would disinhibit an alternative action represented in SC. Our findings suggest that iSPN and iSPN-dependent regulation of ISC implement this computation, allowing animals to optimally navigate the decision landscape.

## Online content

Any methods, additional references, Nature Research reporting summaries, source data, extended data, supplementary information, acknowledgements, peer review information; details of author contributions and competing interests; and statements of data and code availability are available at <https://doi.org/10.1038/s41586-021-04055-4>.

1. Amita, H. & Hikosaka, O. Indirect pathway from caudate tail mediates rejection of bad objects in periphery. *Sci. Adv.* **5**, eaaw9297 (2019).
2. Tai, L.-H., Lee, A. M., Benavidez, N., Bonci, A. & Wilbrecht, L. Transient stimulation of distinct subpopulations of striatal neurons mimics changes in action value. *Nat. Neurosci.* **15**, 1281–1289 (2012).
3. Nonomura, S. et al. Monitoring and updating of action selection for goal-directed behavior through the striatal direct and indirect pathways. *Neuron* **99**, 1302–1314.e5 (2018).
4. Parker, N. F. et al. Reward and choice encoding in terminals of midbrain dopamine neurons depends on striatal target. *Nat. Neurosci.* **19**, 845–854 (2016).
5. Cox, J. & Witten, I. B. Striatal circuits for reward learning and decision-making. *Nat. Rev. Neurosci.* **20**, 482–494 (2019).
6. Kravitz, A. V. et al. Regulation of parkinsonian motor behaviours by optogenetic control of basal ganglia circuitry. *Nature* **466**, 622–626 (2010).

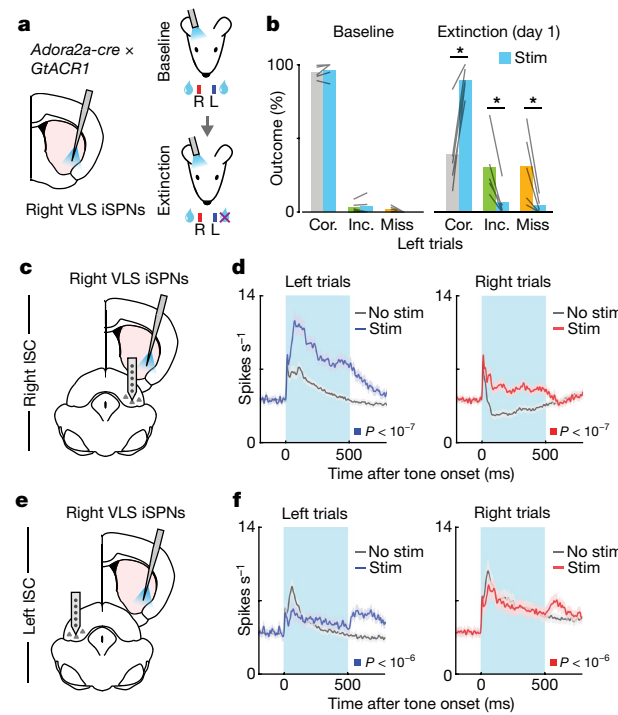


**Fig. 4 | iSPN activity is necessary for suppression of unrewarded action and for exploration of an alternative action.** **a**, Schematic showing a tapered fibre targeting right VLS in an *Adora2a-cre; GtACR1* mouse expressing the inhibitory opsin in iSPN. iSPN in VLS were inactivated during baseline and after extinction on the left spout. **b**, iSPN inactivation significantly increased correct rate and decreased incorrect and miss rates in left trials ( $*P < 0.05$ , two-tailed  $t$ -test) ( $n = 5$  mice). **c**, iSPN in the right VLS were inactivated while an extracellular recording was performed in the right ISC (same side). **d**, Mean firing rate of all directionally selective right ISC units in left- (left) and right- (right) cued trials during stimulation (blue and red) and no-stimulation trials (right ISC = 179 units, 5 mice). The laser-on period is shown in light blue.  $P$ -values shown for stimulation versus no stimulation in the first 100 ms window after laser onset (two-tailed  $t$ -test; Methods). **e, f**, As in **c, d**, for recordings on the left ISC (contralateral of the stimulation side) (left ISC = 166 units, 5 mice).  $P$ -values shown for stimulation versus no stimulation (two-tailed  $t$ -test).

7. Kravitz, A. V., Tye, L. D. & Kreitzer, A. C. Distinct roles for direct and indirect pathway striatal neurons in reinforcement. *Nat. Neurosci.* **15**, 816–818 (2012).
8. Roseberry, T. K. et al. Cell-type-specific control of brainstem locomotor circuits by basal ganglia. *Cell* **164**, 526–537 (2016).
9. Smith, Y., Bevan, M. D., Shink, E. & Bolam, J. P. Microcircuitry of the direct and indirect pathways of the basal ganglia. *Neuroscience* **86**, 353–387 (1998).
10. Sheng, M., Lu, D., Shen, Z. & Poo, M. Emergence of stable striatal D1R and D2R neuronal ensembles with distinct firing sequence during motor learning. *Proc. Natl. Acad. Sci. USA* **116**, 11038–11047 (2019).
11. Bakurin, K. I. et al. Opponent regulation of action performance and timing by striatonigral and striatopallidal pathways. *eLife* **9**, e54831 (2020).
12. Freeze, B. S., Kravitz, A. V., Hammack, N., Berke, J. D. & Kreitzer, A. C. Control of basal ganglia output by direct and indirect pathway projection neurons. *J. Neurosci.* **33**, 18531–18539 (2013).
13. Garr, E. & Delamater, A. R. Chemogenetic inhibition in the dorsal striatum reveals regional specificity of direct and indirect pathway control of action sequencing. *Neurobiol. Learn. Mem.* **169**, 107169 (2020).
14. McPeek, R. M. & Keller, E. L. Deficits in saccade target selection after inactivation of superior colliculus. *Nat. Neurosci.* **7**, 757–763 (2004).
15. Song, J.-H., Rafal, R. D. & McPeek, R. M. Deficits in reach target selection during inactivation of the midbrain superior colliculus. *Proc. Natl. Acad. Sci. USA* **108**, E1433–E1440 (2011).
16. Mana, S. & Chevalier, G. Honeycomb-like structure of the intermediate layers of the rat superior colliculus: afferent and efferent connections. *Neuroscience* **103**, 673–693 (2001).
17. Hikosaka, O., Takikawa, Y. & Kawagoe, R. Role of the basal ganglia in the control of purposive saccadic eye movements. *Physiol. Rev.* **80**, 953–978 (2000).
18. Felsen, G. & Mainen, Z. F. Midbrain contributions to sensorimotor decision making. *J. Neurophysiol.* **108**, 135–147 (2012).
19. Kopec, C. D., Erlich, J. C., Brunton, B. W., Deisseroth, K. & Brody, C. D. Cortical and subcortical contributions to short-term memory for orienting movements. *Neuron* **88**, 367–377 (2015).

20. Kaneda, K., Isa, K., Yanagawa, Y. & Isa, T. Nigral inhibition of GABAergic neurons in mouse superior colliculus. *J. Neurosci.* **28**, 11071–11078 (2008).
21. Rossi, M. A. et al. A GABAergic nigrotectal pathway for coordination of drinking behavior. *Nat. Neurosci.* **19**, 742–748 (2016).
22. Lee, J., Wang, W. & Sabatini, B. L. Anatomically segregated basal ganglia pathways allow parallel behavioral modulation. *Nat. Neurosci.* **23**, 1388–1398 (2020).
23. Shin, J. H., Kim, D. & Jung, M. W. Differential coding of reward and movement information in the dorsomedial striatal direct and indirect pathways. *Nat. Commun.* **9**, 404 (2018).
24. Li, N. et al. Spatiotemporal constraints on optogenetic inactivation in cortical circuits. *eLife* **8**, e48622 (2019).
25. Essig, J., Hunt, J. B. & Felsen, G. Inhibitory midbrain neurons mediate decision making. Preprint at <https://doi.org/10.1101/2020.02.25.965699> (2020).
26. Takahashi, M., Sugiuchi, Y. & Shinoda, Y. Topographic organization of excitatory and inhibitory commissural connections in the superior colliculi and their functional roles in saccade generation. *J. Neurophysiol.* **104**, 3146–3167 (2010).
27. Sookswate, T., Isa, K., Behan, M., Yanagawa, Y. & Isa, T. Organization of GABAergic inhibition in the motor output layer of the superior colliculus. *Eur. J. Neurosci.* **33**, 421–432 (2011).
28. Takahashi, M., Sugiuchi, Y., Izawa, Y. & Shinoda, Y. Commissural excitation and inhibition by the superior colliculus in tectoreticular neurons projecting to omnipause neuron and inhibitory burst neuron regions. *J. Neurophysiol.* **94**, 1707–1726 (2005).
29. Doykos, T. K., Gilmer, J. I., Person, A. L. & Felsen, G. Monosynaptic inputs to excitatory and inhibitory neurons of the intermediate and deep layers of the superior colliculus. *J. Comp. Neurol.* **528**, 2254–2268 (2020).
30. Mysore, S. P. & Knudsen, E. I. A shared inhibitory circuit for both exogenous and endogenous control of stimulus selection. *Nat. Neurosci.* **16**, 473–478 (2013).
31. Mysore, S. P. & Knudsen, E. I. The role of a midbrain network in competitive stimulus selection. *Curr. Opin. Neurobiol.* **21**, 653–660 (2011).
32. Jiang, H., Stein, B. E. & McHaffie, J. G. Opposing basal ganglia processes shape midbrain visuomotor activity bilaterally. *Nature* **423**, 982–986 (2003).
33. Liu, P. & Basso, M. A. Substantia nigra stimulation influences monkey superior colliculus neuronal activity bilaterally. *J. Neurophysiol.* **100**, 1098–1112 (2008).
34. Geddes, C. E., Li, H. & Jin, X. Optogenetic editing reveals the hierarchical organization of learned action sequences. *Cell* **174**, 32–43.e15 (2018).
35. Tecuapetla, F., Jin, X., Lima, S. Q. & Costa, R. M. Complementary contributions of striatal projection pathways to action initiation and execution. *Cell* **166**, 703–715 (2016).
36. Zalocusky, K. A. et al. Nucleus accumbens D2R cells signal prior outcomes and control risky decision-making. *Nature* **531**, 642–646 (2016).
37. Schultz, W., Dayan, P. & Montague, P. R. A Neural substrate of prediction and reward. *Science* **275**, 1593–1599 (1997).
38. Cohen, J. Y., Haesler, S., Vong, L., Lowell, B. B. & Uchida, N. Neuron-type-specific signals for reward and punishment in the ventral tegmental area. *Nature* **482**, 85–88 (2012).
39. Iino, Y. et al. Dopamine D2 receptors in discrimination learning and spine enlargement. *Nature* **579**, 555–560 (2020).
40. Yamaguchi, T. et al. Role of PKA signaling in D2 receptor-expressing neurons in the core of the nucleus accumbens in aversive learning. *Proc. Natl. Acad. Sci. USA* **112**, 11383–11388 (2015).
41. Lee, S. J. et al. Cell-type-specific asynchronous modulation of PKA by dopamine in learning. *Nature* **590**, 451–456 (2021).

**Publisher's note** Springer Nature remains neutral with regard to jurisdictional claims in published maps and institutional affiliations.

© The Author(s), under exclusive licence to Springer Nature Limited 2021

# Article

## Methods

### Mice

All mouse handling and manipulations were performed in accordance with protocols approved by the Harvard Standing Committee on Animal Care, following guidelines described in the US National Institutes of Health Guide for the Care and Use of Laboratory Animals. For behavioral experiments, we used male and female (3–6 months old) *Adora2a-cre*<sup>42</sup> (B6.FVB(Cg)-Tg(Adora2a-cre)KG139Gsat/Mmucl, 036158-UCD) from C57BL/6J backgrounds acquired from MMRRC UC Davis. For muscimol infusion experiments (Extended Data Fig. 4d) and ISC/IRt jaws inhibition experiments (Fig. 3, Extended Data Fig. 6c–f), wild-type (C57BL/6NCrl, Charles River) mice (2 months old) were used. For iSPN inhibition experiment (Fig. 4), used male and female (-2 months old) *Adora2a-cre* mice crossed with *R26-CAG-LNL-GtACR1-ts-FRed-Kv2.1*<sup>24</sup> reporter mouse (The Jackson Laboratory, stock no. 033089). For the dSPN inhibition experiment (Extended Data Fig. 3), we used male and female (-3 months old) *Drd1a-cre*<sup>42</sup> mice (B6.FVB(Cg)-Tg(Drd1-cre) EY262Gsat/Mmucl, 030989-UCD) crossed with *R26-CAG-LNL-GtACR1-ts-FRed-Kv2.1* reporter mouse. All transgenic mice used for experiments were heterozygous for the relevant *cre* allele. Mice were housed on a 12 h:12 h dark:light reversed cycle.

### Surgery and viral injection

All mice underwent headpost–fibre surgery before training, and craniotomy surgery after training, prior to electrophysiology. This minimized the duration of brain surface being exposed. Mice were anaesthetized with isoflurane (2.5% in 80% oxygen). Using a stereotaxic frame (David Kopf Instruments, model 1900), the mouse's skull was exposed and levelled (David Kopf Instruments, Model 1905). The patch of skin covering the skull was cut and removed. A craniotomy with diameter ~300 µm was made with a drill (David Kopf Instruments, Model 1911) for each viral injection. Viruses were injected using a pulled glass pipette (Drummond Scientific Company pipettes) that was cut with bevel (~30°, 35–50 µm inner diameter), and a syringe pump (Harvard Apparatus, 84850). Viruses were frontloaded at a rate of 500 nl min<sup>-1</sup>, and the pipette was lowered slowly into the target region. The pipette was first lowered 300 µm deeper than the target dorsoventral coordinates. The pipette was left in the brain for 5 min before injection began, at a rate of 75 nl min<sup>-1</sup>. After infusion, the pipette was left in place for a 5 min before it was slowly withdrawn. For fibre implants, a stereotaxic cannula holder (SCH\_1.25, Doric) was used to hold the fibre and slowly lower it into the brain. The fibre and headpost were secured on the skull using Loctite gel (McMaster-Carr, 74765A65) and Zip Kicker (Pacer Technology). A wall surrounding the site of recording was made using Loctite to contain the saline bath for electrophysiology grounding. The site of recording was marked, and the wall was filled with silicone gel (Kwik-Sil, World Precision Instruments). Mice were given pre- and post-operative oral carprofen (MediGel CPF, 5 mg kg<sup>-1</sup> day<sup>-1</sup>) as an analgesic, and monitored for at least 5 days. For craniotomy surgery, the silicon was removed and a craniotomy was made by drilling the skull with a 340-µm-diameter drill bit. The craniotomy was extended 300 µm medial–lateral and anterior–posterior. Care was taken not to damage or puncture dura, as this would result in more infection of the craniotomy.

Viral injection for striatal tapered fibres photostimulation was done in a similar way as previously described<sup>22</sup>. In brief, AAV2/9-hSyn-FLEX-CoChR-GFP (UNC vector core) was injected in the medial and lateral part of striatum (titre: 5 × 10<sup>12</sup> genome copies (gc) per ml, injection volume: 300 nl per site, total 1,200 nl). Lateral striatum virus injection and fibre implant was done at an angle. A total of 4 injections were done spanning the entire striatum. All coordinates were as follows (AP/ML/DV relative to bregma and dura, in mm): DMSVMS: 0.5/1.25/-3.25 and 2.15; DLSVLS: 0.5/3.4/-3.35 and -2.15, at 14.5°; lateral SC: -3.5/1.4/2.25). Two tapered fibres (0.66 NA, emitting length 2 mm, implant length 2.5 mm, Optogenix) were implanted in the right

striatum for mapping the site of biggest effect for iSPN photostimulation experiment (Fig. 1). For all other striatal stimulation experiments, only one fibre was implanted, with the tip targeting VLS.

For Jaws inhibition experiment, we injected AAV9-hSyn-Jaws-KGC-GFP-ER2 (UNC vector core) in either ISC (-3.5/1.4/-2.25) or IRt (-6.4/1/4.25). Coordinates for ISC and IRt were based on projection pattern of VLS recipient SNr (for ISC and IRT, titer: 1.8–3 × 10<sup>12</sup> gc ml<sup>-1</sup>, injection volume: 500 nl per site). For ISC inhibition, either a tapered fibre (0.39 NA, emitting length 1 mm, implant length 1.5 mm, Optogenix) or a cleaved fibre (MFC\_200/230-0.48\_3 mm\_MF1.25\_FL, Doric Lenses) were implanted 250 µm above the injection site. For IRt inhibition, a tapered fibre (0.66 NA, emitting length 2 mm, implant length 2.5 mm, Optogenix) was implanted 250 µm above the injection site.

### Anatomy of SNr and SC projection

We analysed anatomy data from previously published work<sup>22</sup>. In brief, for mapping VLS recipient SNr projection (Extended Data Fig. 4a–c), -75 nl of AAV2/1-hSyn-Cre (1 × 10<sup>13</sup> gc ml<sup>-1</sup>, University of Pennsylvania Vector Core or Addgene AV-1-PV2676, titre: 1 × 10<sup>13</sup> gc ml<sup>-1</sup>) was injected into VLS (+0.5/2.25/-3). This was followed by an injection of AVV2/1-FLEX-TdTom (University of Pennsylvania Vector Core, titre: 1 × 10<sup>13</sup> gc ml<sup>-1</sup>) into SNr (-3.2/1.5/-4.5). Mice were perfused four weeks after injection. For mapping ISC topography, -150 nl of AAV2/1-hSyn.Flpo (Plasmid from Addgene 60663, packaged at Boston Children Hospital Viral Core, titre: 7.9 × 10<sup>12</sup> gc ml<sup>-1</sup>) was injected into tJM1 (+2.5/+2/-0.25), followed by 100 nl AAV2/1-Ef1a.fDIO.EYFP (Addgene 55641, packaged at Boston Children Hospital Viral Core, titre: 4 × 10<sup>12</sup> gc ml<sup>-1</sup>) in lateral SC (-3.4/+1.5/-2.1). This method allowed us to label the lateral part of SC involved in licking.

### Histology and immunohistochemistry

Mice were euthanized and perfused transcardially with 1 M PBS followed by 4% paraformaldehyde (1 M). After 24 h post-fix in 4% paraformaldehyde, brains were equilibrated in 30% sucrose solution until they sank to the bottom. Brains were then sliced (50-µm-thick) using a cryostat. Slices were mounted on slide glasses with DAPI mounting medium (VECTASHIELD, H-1200) and imaged under a widefield microscope with a 10× objective (VS120 OLYMPUS). In some mice, for localizing the location of the tapered fibres, we immunostained for glial fibrillary acidic protein or GFAP (Agilent Technologies, Z033429-2, 1:500 dilution ratio).

### Behaviour

We designed a lateralized licking task in which mice had to select between two lateralized actions and report their decision by licking the relevant spout instructed by the tone frequency. Mice were head-fixed and placed inside a plastic tube<sup>43</sup>. Each trial began by an ITI during which mice were required to withhold licking. ITIs were chosen randomly between 2,000 and 4,000 ms. Any lick during the ITI reset the clock but did not change the ITI duration. If no licks were detected during the ITI, a 50-ms-duration tone of either low (tone A, 3 kHz) or high (tone B, 12 kHz) frequency was played. Mice had to lick the left spout (tone A) or right spout (tone B), after which a small water drop (1–1.5 µl) was immediately dispensed from the corresponding spout. Not licking within a response window (500 ms relative to tone onset) resulted in a miss trial, and a time out period (6,000 ms). Each session lasted for 45–60 min or until the mouse had multiple consecutive miss trials (~10 miss trials).

Mice were trained in a series of stages in order to reach final expert performance. Mice were first water deprived (up to 85% baseline weight) and habituated to head fixation. This was followed by water delivery on the rig via one of the spouts centred in front of their mouth. A dummy version of the final task was used in which only one tone type was played, with a shorter ITI (1,000–2,000 ms), longer response window (1,000 ms) and shorter time out period (1,000 ms). This version of the task

was meant to teach the mouse to associate the tone with licking. A small water drop was manually dispensed initially when the tone was played to help the training. Mice were then trained to lick sideways by positioning one of the side spouts at the centre initially and gradually moving it to the final position. Mice learned to track the position of the spout and lick sideways within 1–3 days. The same procedure was repeated for both sides, at least two times for each side (each spout ~60 rewards delivery per repetition). Mice were then trained on the final task. Duration of ITI, response window and time out period was gradually adjusted to the final values. During the training phase, we repeated the same tone after an incorrect trial, in order to prevent the mice from learning a strategy of licking only one spout and still collecting rewards.

Mice were trained for at least two weeks (from habituation), after which they were trained until they reached 75% correct performance. For extinction (Fig. 4, Extended Data Fig. 2a–g), mice underwent the same training procedure, after which the one of the spouts was devalued by not dispensing any water reward even after a correct lick. During extinction, we removed timeout period given that mice learned to not lick to the devalued spout. We also trained mice to lick only one spout (Extended Data Fig. 2f, g). Mice underwent the same procedure but were only ever exposed to the left spout throughout training. The right spout was still present and available to the mouse.

### Behavioural setup

Behavioural data were acquired and saved using Arduino (MEGA 2560) and CoolTerm. Licks were detected by recording the voltage drop between the spout and the tube, similar to previously described studies<sup>43</sup>. The inside of the tube was taped with copper foil and grounded. Solenoids (The Lee Company, part number LHQA0531220H) were connected to 20-ml syringes, acting as water reservoirs, and opened for a short duration to deliver water rewards. Water reward size was calibrated by adjusting solenoids opening time (~20 ms). Water delivery spouts were made using blunt syringes needles (18 gauges). They were glued in parallel, separated by 6.5 mm, and connected to the solenoids via tubing (Cole-Parmer, EW-06460-34). A speaker (Madiasound, parts number: tw025a20) connected to an amplifier (FOSTEX, parts number: AP05) was positioned underneath the tube, connected to the Arduino to deliver tones during the task.

In order to monitor the licking behaviour, a CMOS camera (FL3-U3-13S2M-CS, PointGrey) was positioned on the side. A live camera was used to both place the spouts in front of the jaw and monitor behavioural phenotype after photostimulation.

### Photostimulation

We photoactivated iSPN in striatum by expressing CoChR in striatum and delivering blue light (473-nm laser, Optoengine). For functional mapping, two tapered fibres (0.66 NA, emitting length 2 mm, implant length 2.5 mm, Optogenix) were implanted to stimulate a total 8 striatal sites using an optical setup used previously. Only one fibre was stimulated per session (four sites per session). Stimulation was randomly interleaved, and was deployed 20–30% of the time, to minimize persistent behavioural phenotype due to repeated stimulation. We did not observe any gross persistent effect on baseline performance across session due to stimulation. Each photostimulation session consisted of stimulation trials on both left and right trials, across four striatal sites from one fibre. We ran two sessions per fibre per mouse. For other experiments (extinction, one-spout training and extracellular recording), only one fibre was implanted per hemisphere, and only one site (VLS) was targeted for photostimulation. We calibrated the power level for each depth by adjusting the power at the end of the patch cord (before fibre entry) to be 100 µW. Stimulation consisted of a constant 100-ms pulse, delivered 25 ms after tone onset. In order to stimulate distinct depths along the tapered fibre, we used an optical system for delivering different modes of light onto the back of a high-NA patch

cord (0.66 NA) connecting the tapered fibre, similar to the work previously described<sup>22</sup>. A custom code in Matlab was used to control the optical setup via a data acquisition interface (National Instrument) and communicate with the Arduino.

For the ISC and IRT inhibition experiment, we delivered a single pulse of red light (400-ms constant pulse, 8–16 mW, 637 nm) on ~20% of all trials interleaved randomly. For iSPN/dSPN inhibition experiment, we delivered a single pulse of blue light (500 ms, aligned to the onset of the tone onset, constant pulse, 2 mW, 473 nm) on ~20% of all trials interleaved randomly.

For all photostimulation experiments, we checked with a camera position on the side, if the stimulation caused any erratic orofacial behaviour, or whether the stimulation caused mice to protrude their tongue but not reach the spout.

### Electrophysiology

We performed *in vivo* extracellular recoding in ISC while mice were performing the licking task. Mice underwent viral and fibre implant surgery, after which they were trained on the main task for two weeks. Recording mice only received a single fibre in the lateral part, targeting VLS. iSPN in VLS were stimulated to characterize the behavioural phenotype. All recorded mice showed similar behavioural phenotype as reported in previous experiments where only stimulation was performed. One day before the first recording session, one small craniotomy above each lateral SC were made (~0.5 mm in diameter). Care was taken to not remove the dura when drilling through the skull. The craniotomies were covered with silicone gel (Kwik-Sil, World Precision Instruments). During subsequent recording sessions, the silicone gel was removed and the craniotomy was filled with clean saline solution. Sixty-four-channel silicon probes (A2x32-5mm-25-200-177 or A4x16-Poly2-5mm-23s-200-177, NeuroNexus Technologies) were lowered slowly in brain until it reached the target depth (ISC: ~2.2 to ~2.6 mm relative to dura). We explored different location within the craniotomy in order to record from diverse locations within ISC. We dispensed water rewards while lowering the probe and looked for signals locked to rhythmic licking. Cells within a narrow layer spanning about 400 µm around ISC consistently fired in relation to licking. Once reaching the target depth, we left the probes for an additional 5 min for the surrounding tissue stabilize before starting the recording session. For most mice, only a single depth along the tapered fibre (VLS) was stimulated while recording.

We alternated the recoding location of lateral SC (ipsi or contra relative to fibre location) every day and later analysed ISC units separately based on recording location (Fig. 2, 4). We performed recording until the craniotomies became too unhealthy to record from, performance degraded due to repeated insertion of the silicon probe, or the number of observable units in ISC dramatically decreased (range: over 2 weeks). During the last session, we marked the centre of the craniotomy with probes coated with Dil and later confirmed the recording location in histological slices.

Signals were acquired through OmniPlex Neural Recording Data Acquisition System (Plexon). Signals from each channel were filtered (analogue filter 0.1–7,500 Hz; digital filter 0.77 Hz high pass), digitized at 40 kHz, and single units were manually sorted using Offline Sorter (v3.3.5, Plexon). Units were first detected using a hard threshold (below ~44.63 µV). Neighbouring channels were grouped into tetrodes to aid sorting. Principal component feature space was visually inspected and used to manually draw boundaries of each putative single unit cluster. Artefacts due to spout contact were clearly visible in all channels and easily removed using non-linear energy/energy dimension.

### Muscimol infusion

We infused muscimol (Sigma-Aldrich) in lateral SC unilaterally while mice were performing the lateralized licking task (Extended Data Fig. 4d). A craniotomy (~0.6-mm diameter) was made above each

# Article

lateral SC one day before muscimol infusion. We used a glass pipette frontloaded with muscimol via a syringe pump (see ‘Surgery and viral injection’). While the mouse was head-fixed, the silicone gel above the craniotomy was removed and the injection pipette was slowly lowered into the target depth (2,200  $\mu\text{m}$  below dura). The pipette was left in the brain for 5 min before starting the behavioural session. When the mouse had performed 200–250 trials, we started infusing muscimol<sup>21</sup> (450–500 ng  $\mu\text{l}^{-1}$ ) at a rate of 50 nL  $\text{min}^{-1}$  and a total volume of 100–150 nL. All mice displayed licking deficit within the first 5 min of the start of infusion. We compared the performance pre- and post-muscimol infusion. For post-muscimol infusion trials, we analysed the last 200 trials of the session to take into account the time for muscimol to diffuse in the tissue. After 1 h, we aborted the session, the pipette was slowly raised, and the craniotomy was covered with fresh silicone gel. Some mice received a mixture of muscimol and cholera toxin subunit B (recombinant)-Alexa Fluor 647 conjugate (Thermo Scientific) to localize the site of infusion. All mice fully recovered from previous muscimol infusion session and no performance deficit was observed on the next session, during pre-infusion control trials. At one infusion site, we noticed that baseline performance was low from the beginning, possibly owing to damage from the infusion pipette being lowered into the brain. Each mouse received two infusion sessions (one per site), and all sessions were combined for the analysis.

## Behavioural data analyses

We categorized each trial outcome as correct, incorrect or miss. Correct trials were trials in which mice licked the correct spout (tone A, left; tone B, right) within a response window (500 ms). Incorrect trials were trials in which mice licked the wrong spout. Miss trials were trials in which mice did not initiate any licks within the response window. We quantified the mouse’s performance by counting the fraction of correct, incorrect and miss trials for a given session (Fig. 1).

The functional map of striatal site effective at changing behaviour was determined using hierarchical bootstrapping to account for variability across mice, sessions and trials (Fig. 1e, Extended Data Fig. 1d). We tested against the null hypothesis that the stimulation did not change the fraction of correct/incorrect/miss trials. In each round of bootstrapping, we re-sampled data by separately replacing from mice, sessions within each mouse, and trials (both stim and no-stim trials shuffled) within each session. We then computed the performance change on the re-sampled data set. Bootstrapping 10<sup>5</sup> times produced a distribution of performance changes that reflected the behavioural variability, and the one-tailed *P*-value was the fraction of times in which bootstrapped data produced equal or greater change in performance than that observed. To compare performance changes after VLS iSPN stimulation, we performed *t*-test (two-tailed) on the percentage outcome for stim and no-stim trials across all sessions. For extinction experiment, for each mouse, we quantified the fraction of correct/incorrect/miss trials during stim/no stim trials for left and right trials, and before/after extinction. We ran at least two stimulation sessions for each condition (pre- vs post-extinction) and averaged the percentage outcome across sessions. To test if extinction changed the probability of licking incorrectly, we first computed the change in incorrect rate after stimulation ( $\Delta$ incorrect) to account for baseline incorrect rate and compared it before and after extinction.

## Electrophysiological data analyses

We collected extracellular recording data for iSPN activation experiments from 7 mice, 71 individual sessions, comprising of 617 units (left SC/right SC = 294/379). For ISC inhibition experiments, data came from 4 mice, 29 individual sessions, comprising of 252 units. For iSPN inhibition experiments, data came from 5 mice, 47 individual sessions, comprising of 503 units (left SC/right SC = 224/279).

All units were pooled together for analysis. We smoothed the firing rate traces with a gaussian window for display purposes (individual

units: 20-ms window, mean across units: 10-ms window). For each unit, we determined its coding preference (contra preferring vs ipsi preferring) by comparing the spike count in the first 100-ms window after tone onset during left vs right correct trials (two-tailed *t*-test, *P* < 0.05). Each unit was categorized into contra preferring, ipsi preferring, or no preference if it did not pass the *P*-value threshold. Contra and ipsi preferring units were termed ‘selective units’. To compute selectivity, for each unit we computed the mean firing rate during preferred minus anti preferred trial type. Selectivity was then averaged across units to give a measure of population selectivity (Fig. 2c). To test for bias in the population selectivity, we compared spikes count during ipsi vs contra in a 200-ms window after tone onset (Extended Data Fig. 4f). Coding preference could reflect distinct cell type within SC (for example, excitatory vs inhibitory). However, we did not observe any difference in spike waveform features, although contra-preferring units tended to have higher mean firing rate (Extended Data Fig. 4j).

To quantify the effect of stimulation on ISC activity, we grouped all units recorded on the left SC or right SC and computed the change in firing rate after stimulation ( $\Delta$ spikes per s = no stim spikes per s – stim spikes per s). We quantified whether the effect of stimulation was significant by comparing the spike counts during the stimulation window (100 ms) vs control window (25–125 ms relative to tone onset for iSPN activation and ISC inhibition, 0 ms–100 ms for iSPN inhibition). The first 100-ms window was chosen given that mice took on average at least 100 ms to contact the spout with the tongue (Extended Data Fig. 1c). Thus, activity during this window is unlikely to reflect pure efference copy, but rather activity causal to upcoming behaviour. Each unit was categorized into significantly excited, inhibited, or no change (Extended Data Fig. 4f). The above analyses were done only for all selective units.

To test whether the ISC activity after stimulation could predict behavioural outcome, we analysed a subset of sessions during which we had more 5 trials for each outcome (miss and incorrect). We compared the spike counts during the 100-ms stimulation window vs control window (25–125 ms relative to tone onset) (Extended Data Figs. 5c, 6l). A similar analysis was performed for the iSPN inactivation experiment (Extended Data Fig. 7f). For left trials, we tested whether changes in ISC activity could predict left lick vs no lick. For right trials, we tested whether changes in ISC activity could predict left lick vs right lick.

In a subset of *Adora2a-cre* mice used for initial behavioural experiments (4 out of 7), we stimulated iSPN during the ITI period. This allowed us to test the effect of stimulation on ISC activity at resting state without the interaction with the tone. We conducted similar analysis as above, to test whether the ISC activity after iSPN stimulation could predict behavioural outcome by analysing the spikes count during the stimulation window (Extended Data Fig. 5e–g).

## Dimensionality reduction

We applied targeted dimensionality reduction technique similar to previous studies in order to understand the effect of stimulation on ISC activity<sup>44,45</sup>. We assumed all *n* units from different sessions or mice could have been recorded simultaneously and were pooled together to make a trial-averaged matrix  $\mathbf{x}$  ( $n \times t$  dimensions) aligned to the first lick, with each row representing a single unit, and each column representing a single time bin. We found an  $n \times 1$  vector, in the *n*-dimensional activity space that maximally separated the response vectors in correct lick left trials ( $\mathbf{x}(t)_{\text{left}}$ ) and correct lick right trials ( $\mathbf{x}(t)_{\text{right}}$ ), termed the coding direction ( $\mathbf{CD}$ ).  $\mathbf{CD}$  was computed by subtracting the activity of left – right trials during a 200-ms window centred around the time of first lick (−100 to +100 ms relative to spout contact), and divided by its length, giving a unit vector  $\mathbf{CD}$ . Projecting activity along  $\mathbf{CD}$  ( $\mathbf{CD}^T \mathbf{x}$ ) allowed us to separate trajectory for left vs right trials (Extended Data Figs. 8c, 9c). By construction,  $\mathbf{CD}^T \mathbf{x}$  was positive during left trials. Although  $\mathbf{CD}$  was computed using the time

of first lick, we used activity  $\mathbf{x}$  aligned to tone onset for computing projections, to make comparison between stimulation and no-stimulation trials easier. Separability for trial type was defined as the difference between left vs right trials projection along a specific dimension (for example, **CD**). We also explored different time windows for the choice of **CD** (0–100 ms relative to tone onset, −100 to 0 ms relative to spout contact), and obtained similar separability for left vs right trials (Extended Data Fig. 9a, c).

In order to capture the remaining variance in the data, we built a matrix consisting of trial-averaged activity for  $n$  units during left and right trials, with  $t$  time bins. Left and right trials were concatenated, giving a  $n \times 2t$  matrix. We then removed the component along **CD** by subtracting the projection along **CD** giving  $\mathbf{x}_{\perp CD} = \mathbf{x} - (\mathbf{CD})(\mathbf{CD}^T \mathbf{x})$ , which is the subspace orthogonal to **CD**. We then applied standard principal component analysis (PCA) to this  $\mathbf{x}_{\perp CD}$ , giving PCs that capture variance orthogonal to **CD**. We used time points −400 to +400 ms relative to tone onset for PCA. Data was centred, but not normalized, thus preserving differences in firing rate across units. Only correct control trials were used to compute the **CD** and **PCs**. We also tried to use PCA without computing and subtracting **CD**. This gave similar results as the approach mentioned above, with **PC2** separating left vs right correct trials.

To understand the effect of iSPNs stimulation on ISC activity, we projected stimulation trials activity matrix onto different dimensions (**CD**, **PC1–PC5**). Importantly, stimulation trials were not used to compute different dimensions. To quantify the magnitude of stimulation along specific dimensions, we computed the difference between stimulation and no-stimulation trial projection along specific dimensions (Extended Data Fig. 9b). We took all correct/incorrect/miss trials for no stimulation trials, in order to make stim vs no stim comparison fair. For iSPN inactivation, we computed **CD** by taking the left trials stimulation correct trials and right trials no-stimulation trials. This was because extinction caused mice to no longer lick during left no-stimulation trials. For iSPN inactivation, we computed **CD** by taking the correct left stimulation trials and right trials control trials. This was because extinction caused mice to no longer lick during control trials (Extended Data Fig. 8d).

All error bars for projections along lower dimensional space were computed using bootstrapping across units. Every bootstrap consisted of resampling units with replacement and computing **CD** and **PCs** de novo (5,000 times).  $P$ -values were the fraction of times a bootstrap resulted in the opposite sign of that experimentally obtained. PCA results after bootstrapping can be unstable (sign flipping) owing to the indeterminacy of the sign of PCA loadings. We used an approach previously described<sup>46</sup> to assign a sign to **PCs** that most resemble the direction of the data after each bootstrap. For each **PC**, we changed the sign of the **PC** so that the sum over the dot product of the **PC** and data points would be greater than zero:  $\sum_{t=0}^T \mathbf{PC}_t \cdot \mathbf{x}(t) > 0$ . For each **PC**, we explored and chose different timepoints that did not result sign flipping.

## Software and statistical analyses

Custom Matlab (2016b) code and Arduino code was used to collect behavioural data and slice physiology data. OlyVIA 2.9/ImageJ1.46r was used to process and analyse histology data. FlyCapture2 was used to monitor behaviour. OmniPlex1.16.1 was used to acquire Ephys data. Matlab (2016b) and Excel16.38 was used to analyse all data. Offline Sorter v3.3.5 was used to sort spikes for ephy data.

All statistical analyses were performed using custom code written in Matlab. We used two-tailed *t*-test for all statistical comparisons unless stated otherwise. For functional mapping of striatum (Fig. 1e), we used bootstrap (see ‘Behavioural data analyses’ and ‘Dimensionality reduction’). The significance level was not corrected for multiple comparisons. No statistical methods were used to predetermine sample sizes, but our sample sizes are similar to those reported in previous publications. Data distribution was assumed to be normal, but this was not formally tested.

## Schematics

Mouse diagram was modified with permission from the author of a previously published article along with the publisher’s license<sup>47</sup>. Mouse coronal section diagrams were modified from Paxinos Brain Atlas<sup>48</sup>.

## Reporting summary

Further information on research design is available in the Nature Research Reporting Summary linked to this paper.

## Data availability

The data that support the findings of this study are available from the corresponding author upon reasonable request.

## Code availability

The code used for analysis (Matlab) is available from the corresponding author upon reasonable request.

42. Gerfen, C. R., Paletzki, R. & Heintz, N. GENSAT BAC Cre-recombinase driver lines to study the functional organization of cerebral cortical and basal ganglia circuits. *Neuron* **80**, 1368–1383 (2013).
43. Guo, Z. V. et al. Flow of cortical activity underlying a tactile decision in mice. *Neuron* **81**, 179–194 (2014).
44. Mante, V., Sussillo, D., Shenoy, K. V. & Newsome, W. T. Context-dependent computation by recurrent dynamics in prefrontal cortex. *Nature* **503**, 78–84 (2013).
45. Li, N., Daie, K., Svoboda, K. & Druckmann, S. Robust neuronal dynamics in premotor cortex during motor planning. *Nature* **532**, 459–464 (2016).
46. Bro, R., Acar, E. & Kolda, T. G. Resolving the sign ambiguity in the singular value decomposition. *J. Chemom.* **22**, 135–140 (2008).
47. Peron, S. P., Freeman, J., Iyer, V., Guo, C. & Svoboda, K. A cellular resolution map of barrel cortex activity during tactile behavior. *Neuron* **86**, 783–799 (2015).
48. Franklin, K. B. J. & Paxinos, G. *Paxinos and Franklin’s the Mouse Brain in Stereotaxic Coordinates, Compact: The Coronal Plates and Diagrams* (Academic Press, 2019).

**Acknowledgements** We thank members of the Sabatini laboratory and W. Regehr, M. Andermann, N. Uchida and S. Gershman for helpful discussions; J. Levasseur for mouse husbandry and genotyping; J. Saulnier and L. Worth for laboratory administration; and W. Kuwamoto, J. Grande, M. Ambrosino, B. Pryor, E. Lubbers and R. Griep for assistance with behavioural experiments and histology. This work was supported by the NIH (NINDS NS103226, U19NS113201), a P30 Core Center Grant (NINDS NS072030), an Iljou Foundation scholarship and a grant from the Simons Collaborative on the Global Brain.

**Author contributions** J.L. and B.L.S. conceptualized the study, wrote the original draft, and reviewed and edited the manuscript. J.L. performed experiments and analysed the data.

**Competing interests** B.L.S. is a founder of and holds private equity in Optogenix. Tapered fibres commercially available from Optogenix were used as tools in the research.

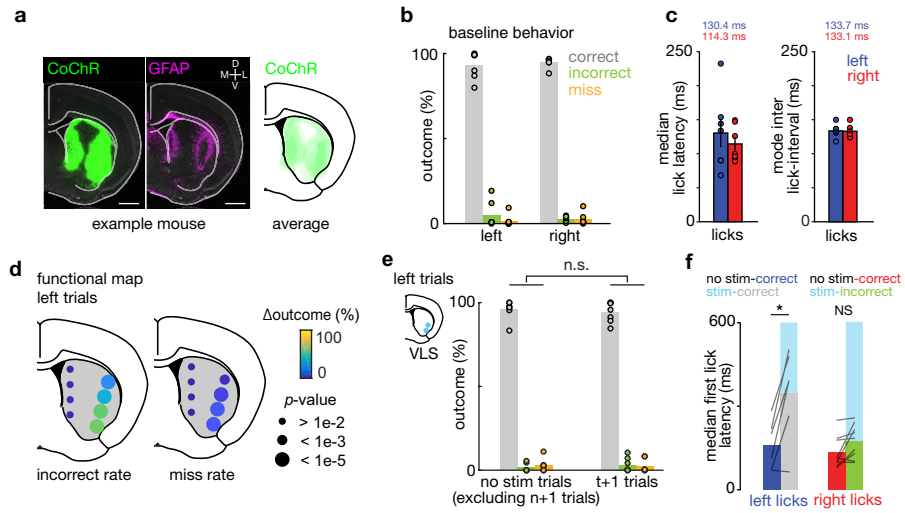
## Additional information

**Supplementary information** The online version contains supplementary material available at <https://doi.org/10.1038/s41586-021-04055-4>.

**Correspondence and requests for materials** should be addressed to Bernardo L. Sabatini.

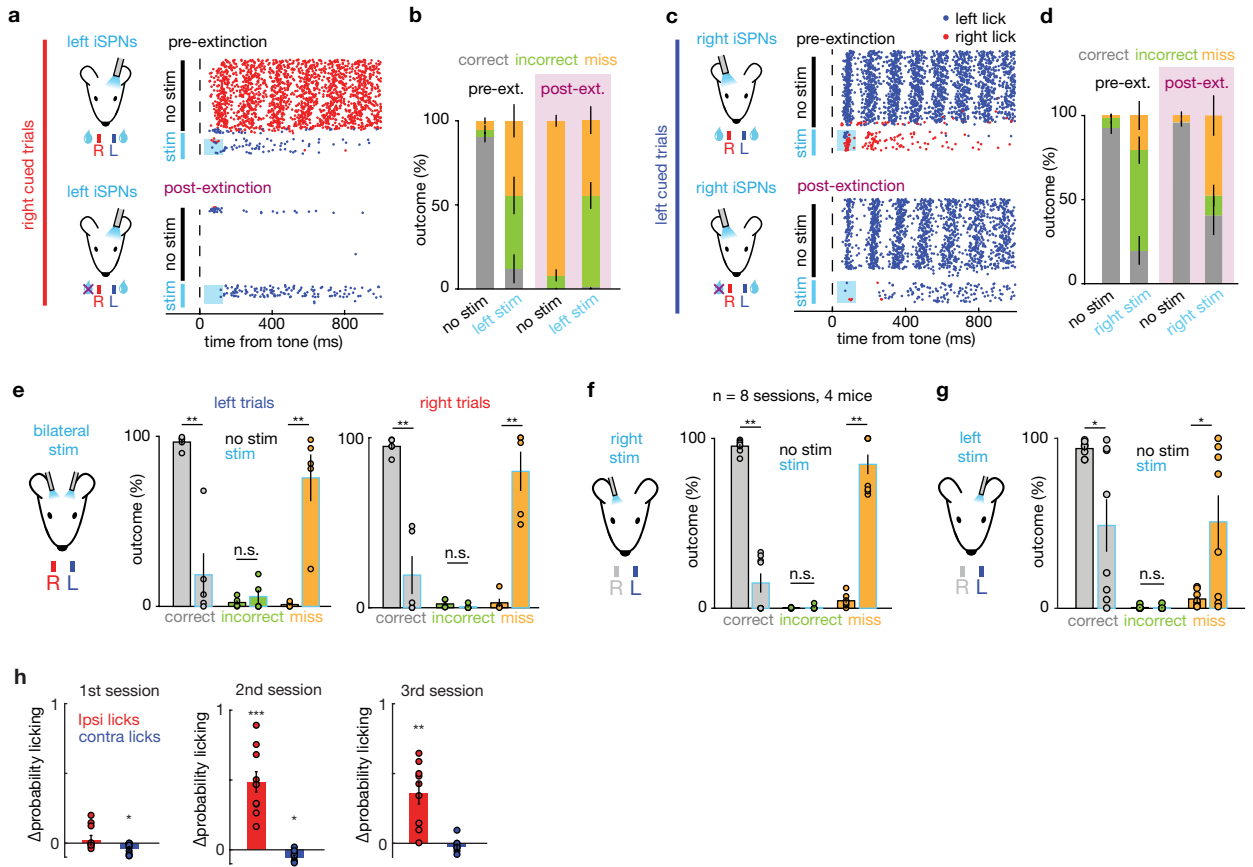
**Peer review information** *Nature* thanks the anonymous reviewer(s) for their contribution to the peer review of this work. Peer reviewer reports are available.

**Reprints and permissions information** is available at <http://www.nature.com/reprints>.



**Extended Data Fig. 1 | Histology, baseline behavior, and effects of iSPN stimulation on the next trial.** **a.** Example histology (left) showing CoChR expression (green) and the tapered fiber location as revealed by glial fibrillary acidic protein (GFAP) staining (magenta). Scale bar: 1 mm. The CoChR expression in striatum averaged across mice is also shown (right). **b.** Baseline expert behavior after two weeks of training. Percentages of correct (grey), incorrect (green) and miss (orange) outcomes for left- and right-cued trials ( $n = 7$  mice). **c.** *left*, Median lick latency measured from tone onset to spout contact for left- (blue) and right- (red) cued trials. *right*, Mode of inter-trial interval for licks to the left (blue) and right (red) ports. **d.** Functional map of optogenetic perturbations at 8 striatal sites showing changes in percentages of incorrect (left) and miss (right) outcomes (see Fig. 1e). The color and size of

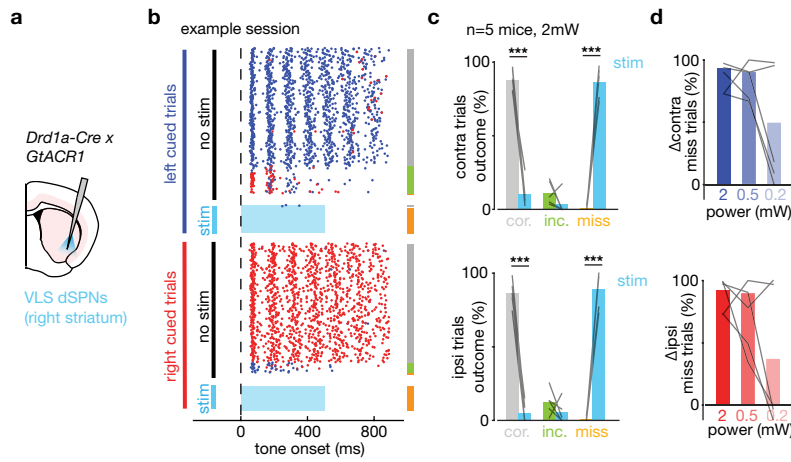
each circle denote the effect size and p-value (bootstrap), respectively ( $n = 5$  mice, 9 sessions). **e.** Effect of VLS iSPN stimulation on the next trial ( $n+1$  trial) relative to control trials (excluding all  $n+1$  trials). For  $n+1$  trials, only those following left-cued trials were included as optogenetic stimulation only affected left-cued trials (i.e. contraversive to the stimulation site in the right striatum) ( $n = 7$  mice) (see Fig. 1e; Methods) (n.s.:  $P > 0.05$ , two-tailed t-test). **f.** Median latency to first lick in no stimulation trials (separated into left vs. right; blue/red) and stimulation trials (sorted into incorrect vs. correct; green/grey). Correct licks during stimulation trials to the left were delayed compared to those during no stimulation trials ( $P < 0.05$ , two-tailed t-test) (left licks:  $n = 6$  sessions, right licks:  $n = 9$  sessions, see Methods).



**Extended Data Fig. 2 | Context-dependent effect of iSPN stimulation.**

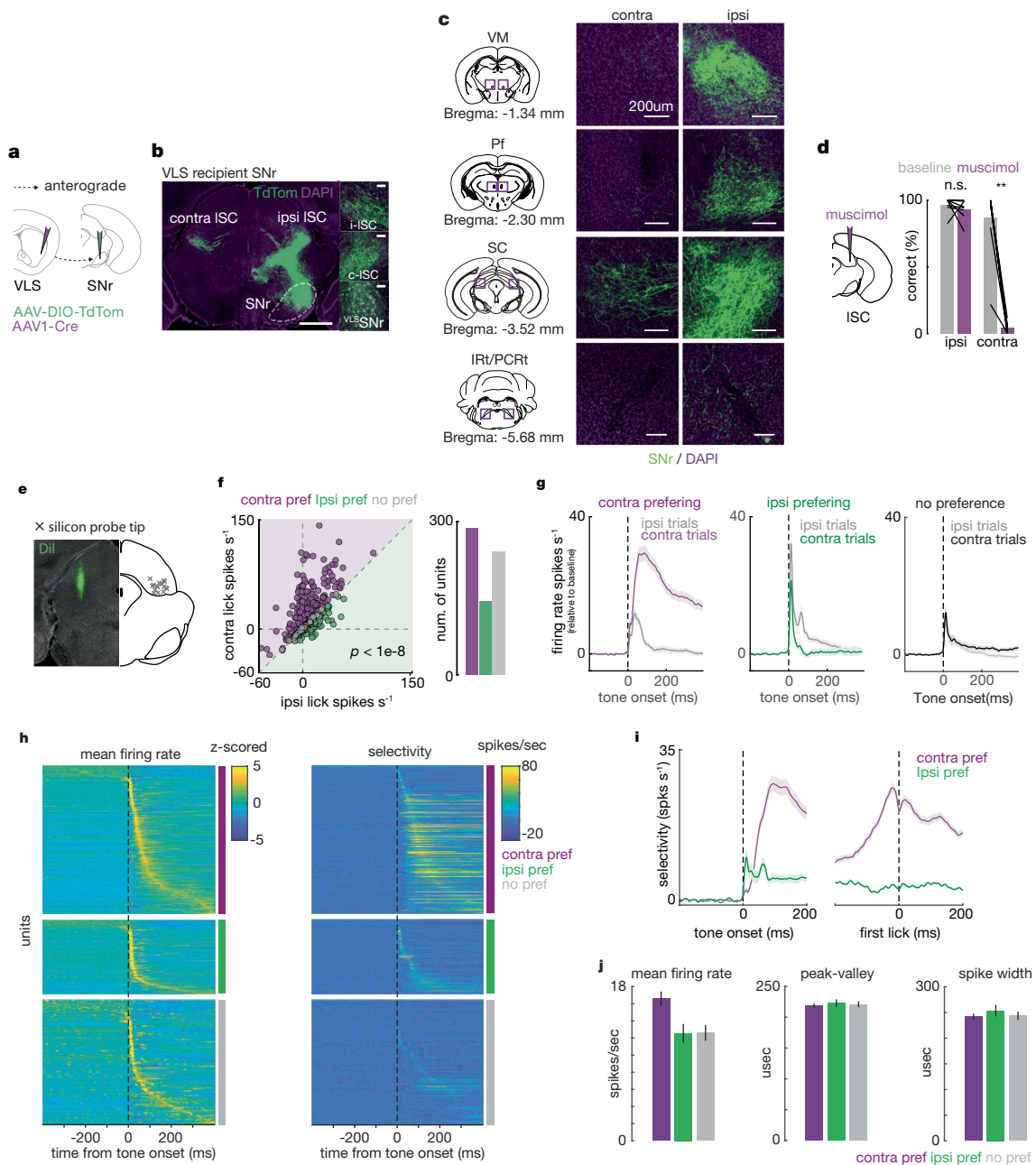
**a, c.** Effect of devaluating one motor program by extinction. An example session from one mouse showing the effects of iSPN stimulation on the left (**a**) or right (**c**) hemisphere before (pre-extinction, top) and after (post-extinction, bottom) devaluation of the right port. Each dot represents licking either to the left (blue) or right (red). Trials (rows) are sorted by being no stimulation (black) and stimulation trials (light blue). Only trials with licking cued to the port contralateral to optogenetic stimulation (right in **a**, left in **c**) are shown. **b, d.** Percentages of each outcome type for pre- (black, left) and post- (purple, right) extinction optogenetic stimulation trials (stim, light blue) and control trials (no stim, black). Outcomes are color-coded grey (correct), green (incorrect), and orange (miss) ( $n = 5$  mice). The selection of the incorrect port following optogenetic stimulation of iSPN on the right striatum significantly decreased after extinction ( $P < 0.0125$ , one-tailed  $t$ -test), whereas it remained the same for iSPN stimulation on the left ( $P = 0.65$ , one-tailed  $t$ -test). **e.** Effect of bilateral iSPN stimulation. Summary plots for the outcomes for no stimulation (black) and stimulation (light blue) trials, during left- (center) and right- (right) cued trials ( $n = 5$  mice). Optogenetic stimulation significantly decreased the correct

outcome rate and increased the miss outcome rate but did not change the incorrect outcome rate ( $**P < 0.001$ , two-tailed  $t$ -test; n.s.:  $P > 0.05$ ). **f. left,** We trained a group of mice to only lick to the left spout, while still having access to both spouts. Right iSPN stimulation in these mice failed to induce licking of the right spout, supporting that stimulation-induced licking is not a hardwired motor program. **right,** Stimulation decreased correct outcome rate and increased the miss outcome rate, but failed to increase incorrect outcome rate (i.e. the rate of licking to the right spout which the mice were never trained to lick) ( $**P < 1 \times 10^{-8}$ , two-tailed  $t$ -test; n.s.:  $P > 0.05$ ). **g.** As in panel **f** for left VLS iSPN stimulation ( $*P < 0.05$ , two-tailed  $t$ -test; n.s.:  $P > 0.05$ ). **h.** In mice trained on the main two-spout task, we also observed that iSPN stimulation during the inter-trial-interval (ITI), when mice rarely licked, induced ipsiversive licking although this effect emerged only after multiple stimulation sessions. Plots showing change in probability of licking after optogenetic stimulation during the ITI relative to control trials ( $n = 10$  mice for 1<sup>st</sup> and 2<sup>nd</sup> session,  $n = 9$  mice for 3<sup>rd</sup> session). Stimulation caused ipsilateral licking from 2<sup>nd</sup> session onward, and weakly suppressed contralateral licking relative to baseline ( $***P < 1 \times 10^{-4}$ ,  $**P < 0.005$ ,  $*P < 0.05$ ).



**Extended Data Fig. 3 | Unilateral inactivation of the direct pathway in VLS suppresses licking on both sides.** **a.** Schematic showing strategy to inhibit striatal direct pathway. Mice expressing an inhibitory opsin GtACR1 in the direct pathway (*R26-CAG-LNL-GtACR1-ts-FRed-Kv2.1* × *Drd1a-Cre*, see methods) was implanted with a tapered fiber in the right VLS. **b.** Example session during which a mouse underwent direct pathway inactivation similar to the

experiment described in Fig. 4b (see Methods). Trials are sorted by trial type similar to that described in Fig. 1d. **c.** Percentage trial outcome for contra trials (top) and ipsi trials (bottom). Unilateral direct pathway inactivation lead to a decrease in correct rate and an increase in miss trial rate ( $P^{***}<0.0005$ , two-tailed *t*-test;  $n=5$  mice, power = 2mW). **d.** Change in miss trials percentage for different power levels (0.2, 0.5 and 2mW).

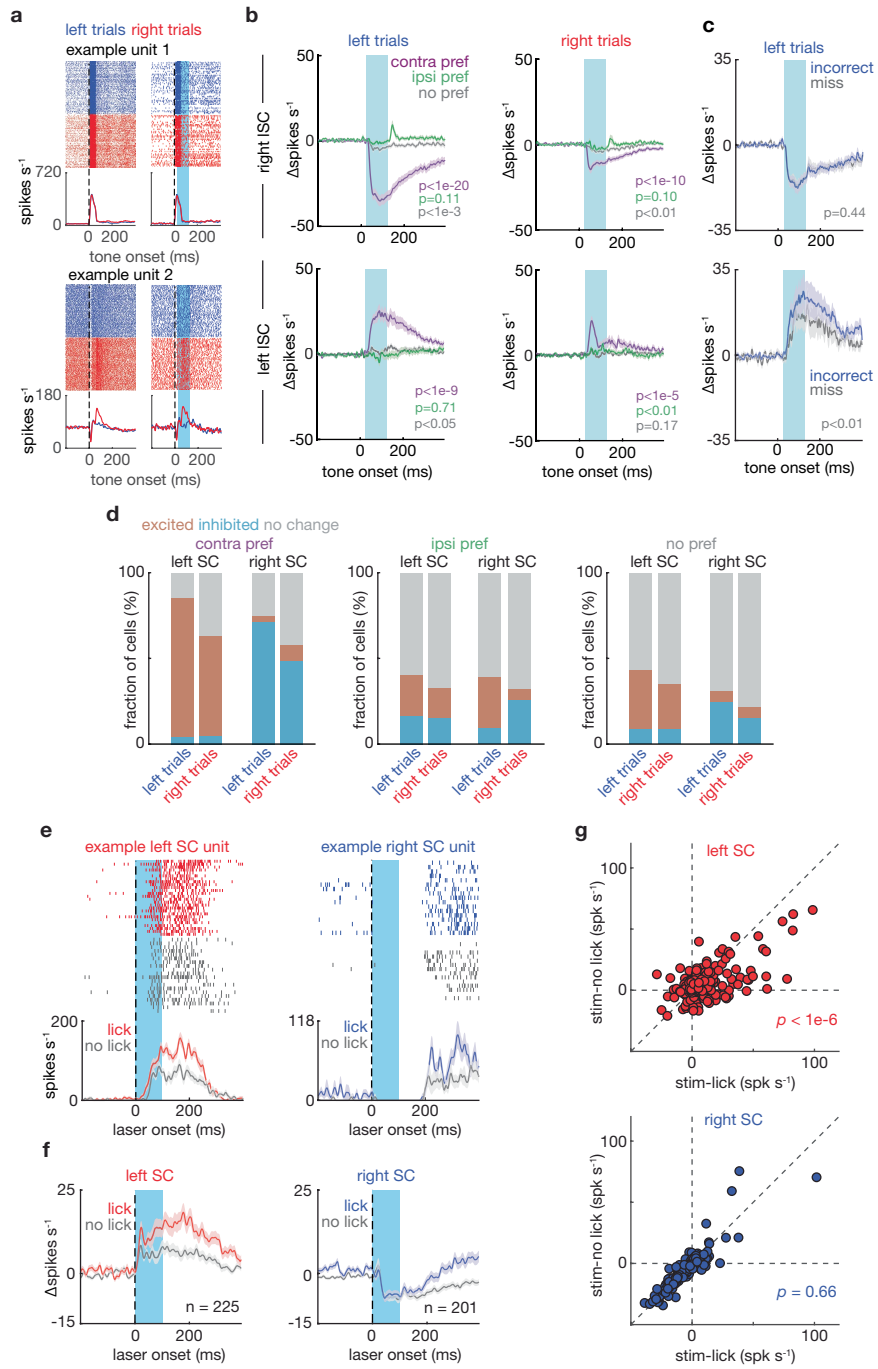


**Extended Data Fig. 4** | See next page for caption.

# Article

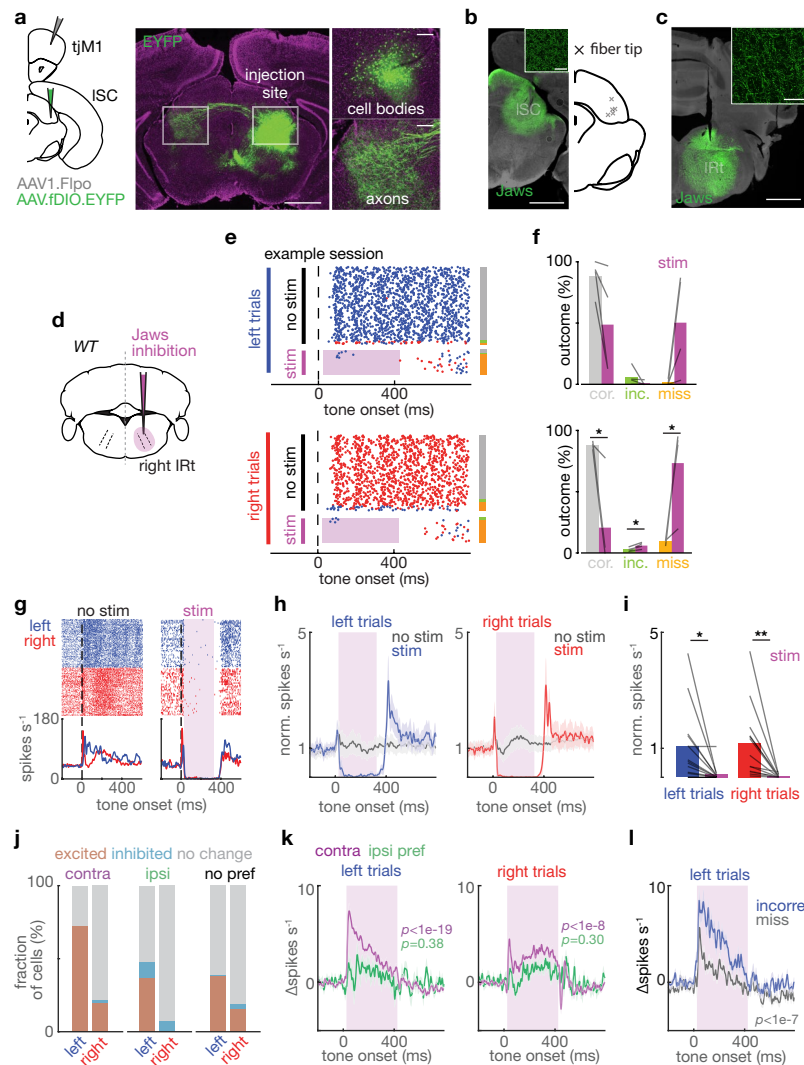
**Extended Data Fig. 4 | VLS recipient SNr projection, effect of muscimol infusion in ISC, and direction selectivity of activity in ISC.** **a-c.** AAV1-Cre mediated anterograde tracing of SNr neurons downstream of VLS shows that VLS recipient SNr (<sup>VLS</sup>SNr) sends bilateral projections to contralateral and ipsilateral ISC. Interestingly, this bilateral projection was largely specific to ISC. **a. left.** Schematic of the AAV1-Cre anterograde trans-synaptic mapping strategy to reveal the projections of VLS-recipient SNr (<sup>VLS</sup>SNr). **b.** Example histology of superior colliculus: <sup>VLS</sup>SNr (green) projects to both ipsilateral ISC (i-ISC) and contralateral ISC (c-ISC). SNr is outlined with a white dotted line. Scale bars: 1mm (left panel), 100  $\mu$ m (3 insets in right column). **c. left column,** Schematics of coronal sections and coordinates relative to bregma. VM: ventromedial thalamus; Pf: parafascicular nucleus; SC: superior colliculus; IRT/PCRt: intermediate reticular formation/parvocellular reticular formation. **right column,** histological examples showing SNr axons (green) labelled via anterograde tracing (see Main text, Fig. 3b) and DAPI (purple). The left and right columns show contralateral and ipsilateral sides, respectively, relative to the labeled SNr cell bodies (i.e. the injection side). Midline crossing SNr axons were only seen in lateral SC. Similar results were observed in total of  $n = 3$  mice. Scale bars: 200  $\mu$ m. **d.** Activity in ISC was necessary for the lateralized licking in the task, as muscimol, a GABA<sub>A</sub> receptor agonist, infused into ISC unilaterally reduced task performance only on trials in which the correct selection port was contralateral to the infusion site. *left*, Muscimol was infused unilaterally in ISC as the mouse performed the task. *right*, percentages of correct trials before (baseline, grey) and after (muscimol, purple) infusion. Muscimol infusion

significantly impaired performance of contralateral cued trials ( $n = 8$  ISC sites, 4 mice,  $P^{**} < 1e-6$ , two-tailed *t*-test). **e. left.** Example histological section showing recording probe location (green = Dil). *right*, location of all probe tip location (cross). Each cross depicts one mouse. **f. left,** Each dot shows the average activity of one unit in the first 200 ms after tone onset (spikes/s) during contraversive trials plotted versus that in ipsiversive trials. The directional selectivity of each unit is color-coded (purple: contra; green: ipsi; grey: no preference). Overall population activity was higher during contraversive trials ( $P < 1e-8$ , two-tailed *t*-test). *right*, Numbers of cells preferring contraversive or ipsiversive licking trials, or having no preference (contra-preferring: 296/673, ipsi-preferring: 139/673, no preference: 238/673). **g.** Mean firing rate of contraversive preferring (purple), ipsiversive preferring (green) and no preference (grey) units shown aligned to tone onset (dashed line) during contralateral and ipsilateral cued trials (contra:  $n = 296$ , ipsi:  $n = 139$ ; mean  $\pm$  s.e.m. across units). **h.** Mean firing rate (z-scored relative to firing during the ITI, left) and selectivity (spikes/s, right) of all ISC units. Each row shows data for a single unit, sorted by coding preference (right column for each panel). For each coding preference, units are sorted by the timing of peak firing relative to baseline. **i.** Selectivity (spikes/s; activity in preferred – anti-preferred trials) aligned to tone onset (left) or 1<sup>st</sup> lick (right) for contraversive- and ipsiversive-preferring neurons (mean  $\pm$  s.e.m across units). **j.** Mean firing rate, peak-valley timing and spike width of waveforms of units in each coding group. No significant differences were observed between groups.



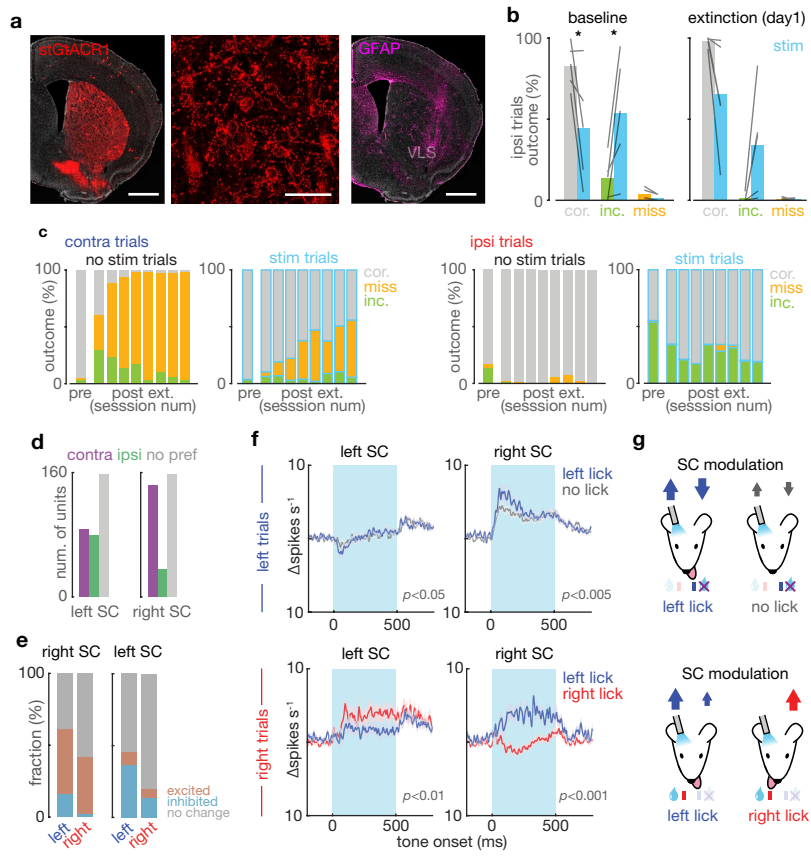
**Extended Data Fig. 5 | Detailed analysis of ISC activity modulation after iSPN stimulation.** **a.** Example units that were not significantly modulated by stimulation. Peri-stimulus histogram showing no stimulation trials (left) and stimulation trials (right, light blue=laser on) during left- (blue) and right- (red) cued trials. **b.** Changes in firing rate (similar as in Fig.2i) but with data separated for contraversive preferring, ipsiversive preferring and no-preference units during left-cued trials (left column) and right-cued trials (right column) in right ISC (top row) and left ISC (bottom row). Only contraversive preferring neurons were significant modulated by iSPN activation in both left and right trials in left and right ISC (p-values for two-tailed *t*-test in the 100ms window after stimulation onset are shown). **c.** Changes in firing rate induced by stimulation ( $\Delta\text{spikes s}^{-1}$ =activity in stim trials – activity in no stim trials) for units in the right (top) and left (bottom) ISC for stimulation trials but including only data from the subset of sessions that had both incorrect and miss outcomes (incorrect: blue, miss: grey; Methods) and separating trials based on outcome. Changes in firing rates in right SC did not differ ( $n=129, P=0.40$ , two-tailed

*t*-test) but changes were larger in left SC during incorrect licking vs miss trials ( $n=64, P=0.01$ , two-tailed *t*-test). Firing rate are show as mean  $\pm$  s.e.m. across units. **d.** Fractions of neurons that were excited, inhibited, or unchanged by optogenetic stimulation in left- and right-cued trials for contraversive-lick-preferring (left), ipsiversive-lick-preferring (middle), and untuned (no pref, right) groups (similar analysis as Fig.2g) recorded in the left or right SC. **e.** iSPN activation during the ITI (e-f). Example units recorded in the left SC (left panel) and right SC (right panel). Peri-stimulus histogram shows trials during which the stimulation did (red/blue) or did not (grey) induce licking. Firing rates are given as mean  $\pm$  s.e.m across trials. **f.** Average changes in firing rate after stimulation ( $\Delta\text{spikes s}^{-1}$ ) in left SC (left panel) and right SC (right panel) grouped by behavioral outcome (red/blue=lick; grey=no lick). Firing rates shown as mean  $\pm$  s.e.m across units (left SC:  $n=225$ ; right SC:  $n=201$ ). **g.** Average firing rates during the 100 ms stimulation window for stimulation trials without (y-axis) vs. with (x-axis) licking. Each dot represents a single unit. P-values show significance of modulation (two-tailed *t*-test).



**Extended Data Fig. 6 | ISC anatomical projection, IRt inhibition, and analysis of ISC/IRt activity after ISC inactivation.** **a.** *left*, Schematic showing strategy to label ISC via anterograde transsynaptic cre (AAV1.Flpo, grey) in tjM1, with injection of anterograde tracer (AAV.fDIO.EYFP, green) in the ISC. *right*, Sagittal section showing the cell bodies around the injection site and the axonal projection on the contralateral ISC. Scale bar, 1 mm (left panel), 200  $\mu$ m (2 insets in right column). **b.** *left*, Coronal section showing expression of Jaws in ISC. Inset shows cell bodies around the injection site. Scale bar, 1 mm (main panel), 50  $\mu$ m (inset in top right corner). *right*, optical fiber tip locations. **c.** Coronal section showing expression of Jaws in IRt. Inset shows cell bodies around the injection site. Scale bar, 1 mm (main panel), 50  $\mu$ m (inset in top right corner). **d.** Schematic illustrating Jaws expression in right IRt in wild type mice. **e.** Example session showing (as in Fig.1d) the effect of IRt inhibition on performance in left and right cued trials, as indicated. The purple rectangle shows the time of laser activation ( $n = 4$  mice). **f.** Quantification of trial outcomes ( $n = 4$  mice). Percentages of correct, incorrect and miss outcomes in no stimulation (grey, green and orange) and stimulation trials (purple) in left (left panel) or right (right panel) cued trials. IRt inhibition caused a significant

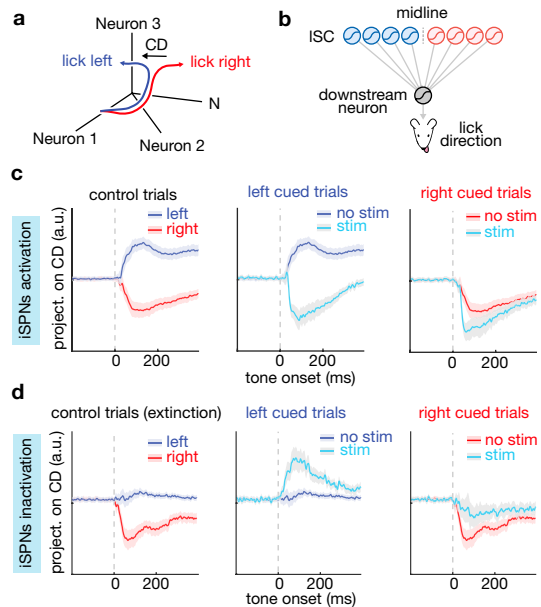
decrease in correct rate ( $P^* < 0.05$ , two-tailed  $t$ -test) and increase in incorrect and miss rates ( $P^* < 0.05$ , two-tailed  $t$ -test) in right trials. **g.** Example unit in ISC that was suppressed via red laser stimulation of Jaws expressed in ISC. Laser on period is shown in purple. **h.** Normalized firing rate of all units recorded during left (left panel) and right (right panel) trials with stimulation (blue/red) and without (grey) stimulation. **i.** Quantification of Jaws inhibition for all units during left (blue) and right (red) trials ( $n = 14$  units;  $P^* < 0.05$ ,  $P^{**} < 0.005$ , two-tailed  $t$ -test). **j.** Fraction of cells that were significantly modulated by contralateral ISC inhibition (similar as in Fig.3j, but repeated for different coding groups). **k.** Changes in firing rate after contralateral ISC inhibition ( $\Delta$ spikes  $s^{-1}$  = activity in stim trials – activity in no stim trials) for ipsiversive- (green) and contraversive (purple) preferring units during left (left panel) or right (right panel) trials. contraversive preferring but not ipsiversive preferring units were significantly modulated by contralateral ISC inhibition ( $p$ -values from two-tailed  $t$ -test shown for each group). **l.** Same as in **h** but sorted by trial outcome (incorrect=blue, miss=grey). ISC activity after contralateral ISC inhibition differentiated incorrect vs miss trials, with higher excitation during incorrect trials ( $P < 1e-7$ , two-tailed  $t$ -test).



**Extended Data Fig. 7 | GtACR1 histology and detailed analysis of effects of iSPN inactivation on task performance and ISC activity.** **a.** *left*, Coronal section showing expression of GtACR1 in striatum in an *Adora2a-Cre* mouse crossed with a conditional GtACR1 mouse (see Methods). *middle*, Inset showing the expression of GtACR1 in iSPN. *right*, Coronal section showing the tapered fiber location as revealed by glial fibrillary acidic protein (GFAP) staining (magenta). Scale bar, 1 mm (left), 50  $\mu\text{m}$  (middle), 1 mm (right). **b.** similar to Fig.4c but for ipsiversive trials relative to fiber location (right trials, see main text) during a baseline session (left) and during extinction day 1 (right). iSPN inactivation caused a significant decrease in correct rate, and significant increase in correct rate during baseline sessions ( $P^*<0.05$ , two-tailed  $t$ -test). **c.** Quantification of percentage trial outcome for contraversive/ipsiversive trials during no stimulation and stimulation trials across session number. **d.** Number of units in each coding group (contra/ipsi/no preference) in left and

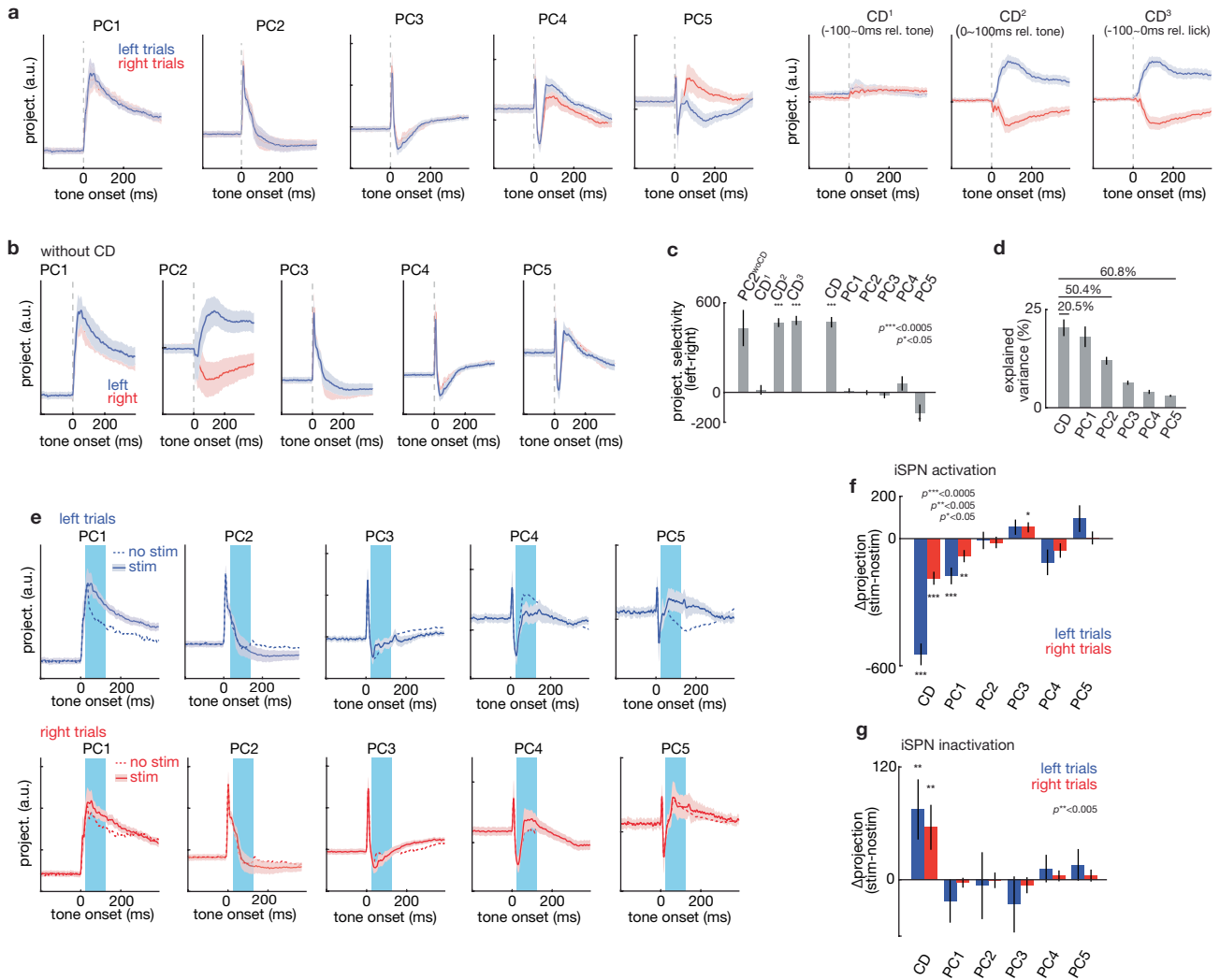
right SC in mice after left spout extinction. **e.** Fractions of units that were significantly modulated (as in Fig.2g). There were more excited than inhibited units in right SC (left trial:  $P<1e-7$ ; right trials:  $P<1e-99$ ; two-tailed binomial test), whereas there were more inhibited than excited units in the left SC (left trial:  $P<1e-7$ ; right trials:  $P<0.05$ ; two-tailed binomial test). **f.** As Fig.4g, but sorted by behavioral outcome (see Main text). Color indicates the behavioral outcome upon iSPN inactivation (blue: left lick; red: right lick; grey: no lick). Change in firing rate in both trial types and both left and right ISC differentiated behavioral outcome ( $p$ -values shown for two-tailed  $t$ -test during 100ms window after laser onset). **g.** Schematic diagram summarizing the results shown in panel e. The size of arrow indicates the relative magnitude of modulation (to be compared only across behavioral outcomes and not across recorded location).

# Article



**Extended Data Fig. 8 | Low-dimensional projection of ISC activity reveals logic of iSPNs modulation of ISC.**

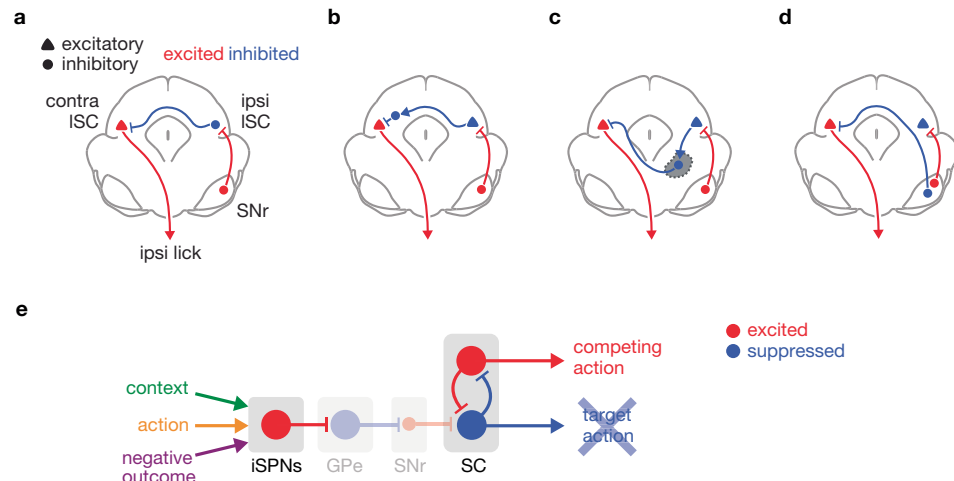
**As the activity of neurons in ISC during the task is complex and heterogeneous, we used dimensionality reduction to examine if, as a whole, neuronal population dynamics in ISC could be related to behavior and help explain effects of iSPN activity manipulation. Using only activity from trials without optogenetic stimulation, we projected ISC activity onto an axis (termed coding direction, CD) that best discriminated upcoming lick choice (see Methods). The projection onto CD represents the linear combination of activity in ISC (as might be calculated by a hypothetical downstream neuron) that allows maximal choice discrimination. As expected, ISC activity along CD discriminated correct trial types (**c**, left panel). Furthermore, optogenetic iSPN activation pushed ISC activity along the CD away from contraversive (left) and towards ipsiversive (right) choice (**c**, middle and right panels), even though activity in the optogenetic trials was not used to calculate the CD. Optogenetic modulation along other dimensions orthogonal to CD (calculated by PCA on the residual non-CD activity) was minimal, indicating that iSPN activity specifically modulates ISC neural population along a trajectory that determines lick choice as opposed to behavioral features, such as lick timing (see Extended Data Fig. 9e, f). After extinction of the left spout, ISC activity no longer moved along the CD towards the left-choice despite delivery of the left cue, consistent with lack of left-port licking in these trials (**d**, left panel). However, after extinction of the left spout, iSPN inactivation pushed ISC activity along the CD towards the left choice (**d**, middle and right panel). Thus, following extinction, activity in VLS iSPN was necessary for suppression of left-choice activity in the ISC. Phrased differently, iSPN activity specifically modulates ISC activity along a choice axis away from an activity space that no longer leads to valuable outcomes. **a**. Schematic showing ISC neural trajectory for left (blue) and right (red) trials. Trajectories maximally diverge along the axis termed coding direction (CD, see methods). **b**. Schematic showing ISC units (circle) on each hemispheres projecting onto a hypothetical downstream neuron (grey circle), which controls lick direction. Projection onto CD can be thought of as activity of a hypothetical neuron whose weights achieve maximal lick choice separation (see methods). **c**. Mean neural trajectories of ISC (both hemispheres combined, see Methods) projected onto CD during iSPNs activation experiment (see Fig. 2, Main Text). Grey dotted line shows the timing of the tone onset ( $t = 0$ ). *left*, Control trials in which mice either licked left (blue) or right (red) without stimulation. *middle*, Left cued trials during no stim (blue) and stim (light blue) trials. *right*, Right cued trials during no stim (red) and stim (light red) trials. **d**. Mean neural trajectories of ISC (both hemispheres combined, see Methods) projected onto CD during iSPNs inactivation experiment after extinction (see Fig. 4, Main Text). Traces plotted as panel **c**.**



**Extended Data Fig. 9 | Detailed analysis of low dimensional projection of ISC activity.** **a.** Activity projections onto PCs, and different coding directions. Left (blue) and right (red) trials are shown relative to tone onset. Coding direction was defined during -100-0ms window relative to tone onset (left, CD<sup>1</sup>), 0-100ms relative to tone (center, CD<sup>2</sup>) and 100-0ms relative to first lick (right, CD<sup>3</sup>) (see Methods). CD<sup>1</sup> was used as a control. **b.** PCA on the original data (without first calculating and removing CD<sup>2</sup> information as in Figure 5). Left/right lick (i.e. choice) information is found in PC2 (2<sup>nd</sup> column). **c.** Left-right choice selectivity measured from the projection of the neural activity along the indicated axes. Selectivity measures how separable the trajectories are along the selected axis. The given P-values are for comparison by one sample two tailed t-test ( $P^{***}<0.0005$ ,  $P^*<0.05$ ). The trajectories are well-separable along different choice axes. PCs did not reliably discriminate trial type compared to CD (except for PC5). **d.** Explained variance along each dimension (see Methods).

CD explained the most variance in the data ( $20.5 \pm 2.3\%$ ). Explained variances for CD, CD+PC1+PC2, and CD+PC1+PC5 are shown. All error bars show bootstrapped standard error across units. **e.** Projections of neural activity as a function of time relative to the tone onset shown along PC3 (left), PC4 (middle) and PC5 (right). Data are shown for left- (top, blue) and right- (bottom, red) cued trials. The dotted lines show activity in no stim trials and thick lines that in stim trials. Light blue rectangle shows stimulation on window. **f.** Changes in activity during the stimulation window (100 ms) for each projection after stimulation ( $\Delta$ project. modulation) along different dimensions during left- (blue) and right- (red) cued trials. Stimulation modulates activity the mostly along CD. P-values show significance of modulation (two-tailed t-test). **g.** similar analysis as panel **f** for iSPN inactivation (Main Fig.4, Extended Data Fig. 8d, see methods). P-values show significance of modulation (two-tailed t-test).

# Article



**Extended Data Fig. 10 | Circuit mechanism of contra ISC excitation, and model of exploration via iSPNs-Colliculus.** **a-d.** Potential circuit mechanisms by which iSPN could excite contra ISC. Color indicates the direction of modulation after iSPN activation, and shapes indicates cell type (triangle: excitatory; circle: inhibitory). Note that all these mechanisms are not mutually exclusive and a combination of these might occur together. We provide evidence for model **a** and **b**, in which inhibition ISC in one hemisphere disinhibit ISC on the opposite hemisphere (Fig. 3). **a.** Long-range inhibitory projection crossing the midline could mediate contra ISC excitation. In this scenario, iSPN will cause SNr to be excited, suppressing ipsi ISC, which in turn will disinhibit contra ISC. **b.** Long-range excitatory projection innervating local inhibitory interneurons could mediate this effect. **c.** A region outside SC (grey patch) could mediate the disinhibitory effect (e.g. nucleus isthmus; see main text).

**d.** Separate population of SNr neurons could innervate ipsi and contra ISC. In this scenario, iSPN activation would lead to bidirectional modulation of SNr neurons, with ipsi ISC projecting SNr neurons being excited, and contra ISC projecting SNr neurons being inhibited. **e.** Schematic diagram of the exploration model proposed. iSPN integrate information about the outcome of specific action performed in a specific context. The function of iSPN to learn which actions lead to a negative outcome and suppress them in the future. iSPN can then suppress the target action that lead to the negative outcome. Via disinhibition within SC, this leads to a rapid execution of a competing motor program. Although the circuit from specific iSPN to target action is hardwired, competitive interaction within SC is more dynamic and tunable so the same activation of iSPN can lead to different actions depending on the availability of the competing motor program.

## Reporting Summary

Nature Portfolio wishes to improve the reproducibility of the work that we publish. This form provides structure for consistency and transparency in reporting. For further information on Nature Portfolio policies, see our [Editorial Policies](#) and the [Editorial Policy Checklist](#).

### Statistics

For all statistical analyses, confirm that the following items are present in the figure legend, table legend, main text, or Methods section.

n/a Confirmed

- The exact sample size ( $n$ ) for each experimental group/condition, given as a discrete number and unit of measurement
- A statement on whether measurements were taken from distinct samples or whether the same sample was measured repeatedly
- The statistical test(s) used AND whether they are one- or two-sided  
*Only common tests should be described solely by name; describe more complex techniques in the Methods section.*
- A description of all covariates tested
- A description of any assumptions or corrections, such as tests of normality and adjustment for multiple comparisons
- A full description of the statistical parameters including central tendency (e.g. means) or other basic estimates (e.g. regression coefficient) AND variation (e.g. standard deviation) or associated estimates of uncertainty (e.g. confidence intervals)
- For null hypothesis testing, the test statistic (e.g.  $F$ ,  $t$ ,  $r$ ) with confidence intervals, effect sizes, degrees of freedom and  $P$  value noted  
*Give P values as exact values whenever suitable.*
- For Bayesian analysis, information on the choice of priors and Markov chain Monte Carlo settings
- For hierarchical and complex designs, identification of the appropriate level for tests and full reporting of outcomes
- Estimates of effect sizes (e.g. Cohen's  $d$ , Pearson's  $r$ ), indicating how they were calculated

*Our web collection on [statistics for biologists](#) contains articles on many of the points above.*

### Software and code

Policy information about [availability of computer code](#)

Data collection Custom Matlab (2016b) code and Arduino code was used to collect data behavioral data and slice physiology data. OlyVIA 2.9/ImageJ1.46r was used to process and analyze histology data. FlyCapture2 was used to monitor behavior. OmniPlex1.16.1 was used to acquire Ephys data.

Data analysis Matlab (2016b) and Excel16.38 was used to analyze all data. Offline Sorter v3.3.5 was used to sort spikes for ephy data.

For manuscripts utilizing custom algorithms or software that are central to the research but not yet described in published literature, software must be made available to editors and reviewers. We strongly encourage code deposition in a community repository (e.g. GitHub). See the Nature Portfolio [guidelines for submitting code & software](#) for further information.

### Data

Policy information about [availability of data](#)

All manuscripts must include a [data availability statement](#). This statement should provide the following information, where applicable:

- Accession codes, unique identifiers, or web links for publicly available datasets
- A description of any restrictions on data availability
- For clinical datasets or third party data, please ensure that the statement adheres to our [policy](#)

The data that support the findings of this study are available from the corresponding author upon reasonable request.

# Field-specific reporting

Please select the one below that is the best fit for your research. If you are not sure, read the appropriate sections before making your selection.

Life sciences       Behavioural & social sciences       Ecological, evolutionary & environmental sciences

For a reference copy of the document with all sections, see [nature.com/documents/nr-reporting-summary-flat.pdf](https://nature.com/documents/nr-reporting-summary-flat.pdf)

## Life sciences study design

All studies must disclose on these points even when the disclosure is negative.

Sample size	No statistical methods were used to pre-define sample size. Our sample size are similar to previous studies (Kravitz, Tye and Kretizer, 2012) that have manipulated striatal activity using optogenetics.
Data exclusions	No data were excluded for the analysis.
Replication	We did not separately replicate the findings using new cohort of mice. However, we report all error bars, p-values for all our data, and our conclusion are based on statistically significant results.
Randomization	Optogenetic stimulation were randomly interleaved during trials using custom Matlab code (Fig. 1). Stimulation sites were also selected randomly during the session using custom Matlab code. There was no need to assign mice to separate groups given that all analysis was based on stim vs no stim trials comparison within mice.
Blinding	Automated scripts were used to run all analysis. There was no need for blinding when allocating mice to groups, given that all analysis was based on stim vs no stim trials within mice.

## Reporting for specific materials, systems and methods

We require information from authors about some types of materials, experimental systems and methods used in many studies. Here, indicate whether each material, system or method listed is relevant to your study. If you are not sure if a list item applies to your research, read the appropriate section before selecting a response.

### Materials & experimental systems

- |                                     |   |
|-------------------------------------|---|
| n/a                                 | Involved in the study   |
| <input type="checkbox"/>            | <input checked="" type="checkbox"/> Antibodies                  |
| <input checked="" type="checkbox"/> | <input type="checkbox"/> Eukaryotic cell lines                  |
| <input checked="" type="checkbox"/> | <input type="checkbox"/> Palaeontology and archaeology          |
| <input type="checkbox"/>            | <input checked="" type="checkbox"/> Animals and other organisms |
| <input checked="" type="checkbox"/> | <input type="checkbox"/> Human research participants            |
| <input checked="" type="checkbox"/> | <input type="checkbox"/> Clinical data                          |
| <input checked="" type="checkbox"/> | <input type="checkbox"/> Dual use research of concern           |

### Methods

- |                                     |   |
|-------------------------------------|---|
| n/a                                 | Involved in the study                           |
| <input checked="" type="checkbox"/> | <input type="checkbox"/> ChIP-seq               |
| <input checked="" type="checkbox"/> | <input type="checkbox"/> Flow cytometry         |
| <input checked="" type="checkbox"/> | <input type="checkbox"/> MRI-based neuroimaging |

## Antibodies

### Antibodies used

We used a Glial Fibrillary Acidic Protein (GFAP) antibody to stain for tapered fiber tracts in striatum (Agilent Technologies, Z033429-2). Dilution of 1:500 was used.

### Validation

The antibody used has been validated by the company (<https://www.agilent.com/store/productDetail.jsp?catalogId=Z033429-2>).

## Animals and other organisms

Policy information about [studies involving animals](#); [ARRIVE guidelines](#) recommended for reporting animal research

### Laboratory animals

Mice. All mouse handling and manipulations were performed in accordance with protocols approved by the Harvard Standing Committee on Animal Care, following guidelines described in the US National Institutes of Health Guide for the Care and Use of Laboratory Animals. For behavioral experiments, we used male and female (3~6 months old) Adora2a-Cre (B6.FVB(Cg)-Tg(Adora2a-cre)KG139Gsat/Mmucl, 036158-UCD) from C57BL/6J backgrounds acquired from MMRRC UC Davis. For muscimol infusion experiments (Extended Data Fig. 4b) and ISC/IRt jaws inhibition experiments (Fig. 3), wild type (C57BL/6NCrl, Charles River) mice (2 months old) were used. For iSPN inhibition experiment (Fig. 4), used male and female (~2 months old) Adora2a-Cre mice crossed with R26-CAG-LNL-GtACR1-ts-FRed-Kv2.1 reporter mouse (The Jackson Laboratory, stock # 033089). For dSPN inhibition experiment (Extended Data Fig. 3), used male and female (~3 months old) Drd1a-Cre mice (B6.FVB(Cg)-Tg(Drd1-cre)EY262Gsat/Mmucl, 030989-UCD) crossed with R26-CAG-LNL-GtACR1-ts-FRed-Kv2.1 reporter mouse. All transgenic mice used for experiments were heterozygous

for the relevant cre allele. Mice were housed on a 12 h/12 h dark/light reversed cycle.

Wild animals

Our study did not involve wild animals

Field-collected samples

Our study did not involve field-collected samples

Ethics oversight

All mouse handling and manipulations were performed in accordance with protocols approved by the Harvard Standing Committee on Animal Care, following guidelines described in the US National Institutes of Health Guide for the Care and Use of Laboratory Animals.

Note that full information on the approval of the study protocol must also be provided in the manuscript.